GEOLOGICA CARPATHICA, DECEMBER 2022, 73, 6, 599–616 https://doi.org/10.31577/GeolCarp.73.6.6

Metabasic rocks from the Zemplinic crystalline basement (Western Carpathians, Slovakia): Metamorphic evolution and igneous protolith

ANNA VOZÁROVÁ[1,✉], ONDREJ NEMEC[1], KATARÍNA ŠARINOVÁ[1] and JOZEF VOZÁR[2]

[1]Comenius University in Bratislava, Faculty of Natural Sciences, Department of Mineralogy, Petrology and Mineral Resources, Mlynská dolina, Ilkovičova 6, 842 15 Bratislava, Slovakia; ✉anna.vozarova@uniba.sk, ondrej.nemec@uniba.sk, katarina.sarinova@uniba.sk
[2]Earth Science Institute of the Slovak Academy of Sciences, Dúbravská cesta 9, P.O. BOX 106, 840 05 Bratislava, Slovakia; jozef.vozar@savba.sk

(Manuscript received March 21, 2022; accepted in revised form July 28, 2022; Associate Editor: Milan Kohút)

Abstract: The Zemplinic pre-Alpine crystalline basement occur within a northwest-southeast striking tectonic horst, uplifted from the basement of the Cenozoic fill of the East Slovakian Basin. Its tectonic affiliation has not yet been clearly resolved, therefore, this either represents a continuation of the Western Carpathians crystalline basement units to the east or belongs to another tectonic unit. The Zemplinic metabasic rocks are represented by typical amphibolites, which are dark-coloured with strong to weakly foliated or lineated structures. The results of geothermobarometry and constructed phase diagrams indicate a P–T interval of an amphibolite facies with conditions of 610–730 °C at 0.58–0.76 GPa. Their critical mineral association Hbl+Pl+Cpx corresponds to the climax of the orogenic metamorphism of the Zemplinic crystalline basement. Based on their chemical composition, the protolith of metabasic rocks corresponds to two volcanic groups: the sub-alkali basalt (Nb/Y = 0.05–0.31) and the alkali basalt (Nb/Y = 0.90–1.85). The Nb_N/Th_N values (= 0.04–0.19) exhibit "arc" signatures for the sub-alkali metabasalts. The sub-alkali metabasalt group, which is shown in the incompatible element's diagrams, indicates that it normalized to N-MORB and E-MORB and inclines to E-MORB basalts, with evidence of Zr–Hf, Ti, Y, and Nb depletion. On the other hand, the group of alkali metabasalts tends to be more transitional to the OIB basalts, with evidence of higher enrichment in LREE and MREE, as well as in Th, U, Nb, Zr, Ti, and Y. The Zemplinic metabasic rocks comprise a variety of enriched basalts, running from intra-oceanic towards within-plate or towards intra-oceanic- and island-arc field accord with the extensional supra-subduction regime of back-arc basins. From the point of view of tectonic development, we consider the Zemplinic Unit to be a continuation of the Inner Western Carpathians.

Keywords: metabasic rocks, petrology, geochemistry, P–T conditions, genesis

Introduction

The Zemplinic Unit, which is situated on the boundary of the Slovak Republic and Hungary (Fig. lA), is said to represent the easternmost tectonic unit of the Central Western Carpathians (Slávik 1976). The basement rocks are exposed in a small area in the south-eastern part of Slovakia, crossing the border with Hungary (ca. 6 km long and 2 km wide; Pantó 1965; Baňacký et al. 1986, 1989; Fülöp 1994) (Fig. 1A, B). Occurrence of crystalline basement rocks under the Late Paleozoic and Neogene–Quaternary sedimentary cover has been confirmed by several boreholes in both the Slovak and Hungarian territories (Pantó 1965; Grecula & Együd 1982; Vozár et al. 1986).

As a result of the position of this unit between the Western and Eastern Carpathians, as well as from some Proterozoic age data obtained from basement rocks (Pantó 1965), its relations to the Western or Eastern Carpathians are speculative (Slávik 1976; Rudinec & Slávik l970; Maheľ 1986; Grecula et al. 1981a; Plašienka 2018 and references therein). Although it has been correlated with the Western Carpathians' crystalline zones by several authors (Andrusov 1968; Fusán et al. 1971; Maheľ 1986; Vozárová & Vozár 1988; Vozárová 1991; Faryad 1995; Faryad & Balogh 2002; Vozár et al. 2010), the Zemplinic Unit represents a continuation of the Central Western Carpathian crystalline basement units to the east. From the findings of other authors, the structure of the Zemplinicum indicates a rather independent position within the Carpathian units. Its connections toward the Mecsek zone of the Tisia Terrane were suggested by Grecula & Együd (1977) and Plašienka et al. (1997).

Since the surface outcrops are rare and strongly-weathered, we only present petrological information from the crystalline basement rocks of the samples from the BB-1 borehole, which is situated near the former Byšta health spa (Vozár et al. 1986). For petrological analysis, we used the amphibolite samples from nine horizons in the borehole (Fig. 1C). The main objective was to determine the evolution and pressure–temperature conditions of regional metamorphism and the genesis of source magma on the basis of whole-rock chemical analyses, as well as chemical analyses of critical mineral associations. We will also try to bring new evidence to address the tectonic position of the Zemplinic Unit, regardless of whether it is part of the Western Carpathian orogenic system or not.

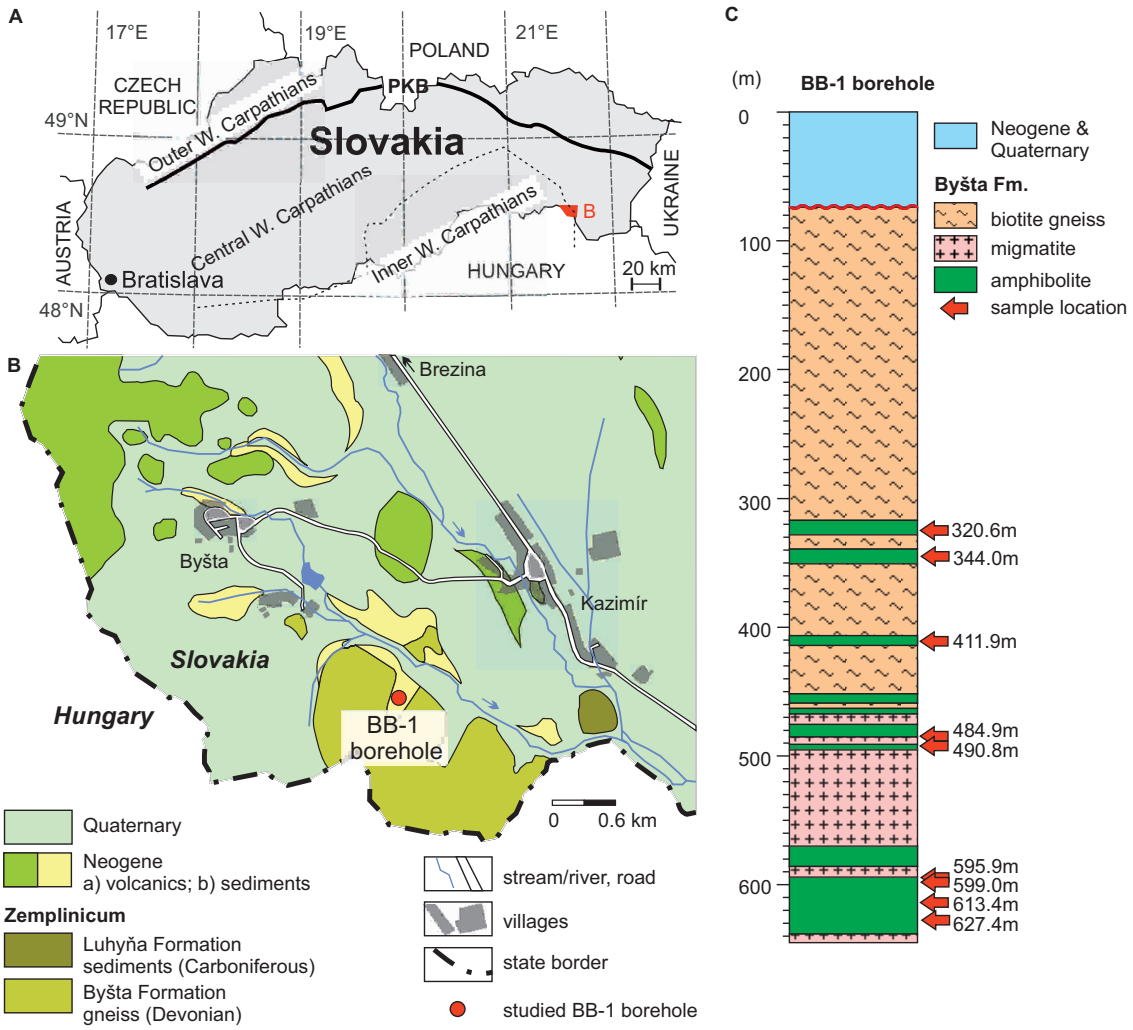

Fig. 1. A — Studied area location in the simplified map of Slovakia; **B** — Geological map of the considered area showing the BB-1 borehole location, modified according to the Geological map of southern part of the East Slovakian Lowland, 1:50 000, from Baňacký et al. (1986); **C** — Schematic lithological column of the BB-1 borehole with the studied sample locations.

Geological framework

The Zemplinic basement rocks, together with their Late Paleozoic and Mesozoic–Cenozoic successions of cover, occur within a northwest-southeast striking tectonic horst, uplifted from the basement of the Cenozoic fill of the East Slovakian Basin (Fig. 1). The surface occurrence of the crystalline basement is known in the area west and southwest of the village of Michaľany (Byšta Horst in the sense of Baňacký et al. 1989), the continuation of which is also evident in the Hungarian territory and further in the basement of the Cenozoic sedimentary basin fill. The most common surface rocks are light quartz–muscovite blastomylonites, which form the Lysá Hora and the Veľká Hora Hills. Amphibolites and biotite gneisses are present on the northwestern flank of Lysá Hora Hill. Basement rocks under the Upper Carboniferous/Mesozoic to Cenozoic cover sequences were also found in 12 deep boreholes, both in the Slovakian and Hungarian territories (Pantó 1965; Grecula et a1. l981b; Vozár et al. 1986).

In general, the Zemplinic basement consists of various types of biotite paragneisses (irregularly with sillimanite, staurolite, garnet, and kyanite), locally intercalated with amphibolites, orthogneisses, and migmatites (Pantó et al. 1967; Magyar 1969; Kisházi & Ivancsics 1988; Vozárová 1991; Faryad 1995; Faryad & Vozárová 1997; Faryad & Balogh 2002). On the basis of their mineral composition, two groups of paragneisses have been distinguished: kyanite-bearing and kyanite-free. Rare pebbles of granitoid rocks, which were likely a former integral part of this basement, have been described within the overlapping Pennsylvanian and Permian conglomerates (Együd 1982; Vozárová & Vozár 1988; Faryad 1995). Additionally, low-grade metamorphic rocks (phyllite, metarhyolite) have been reported from the boreholes Felsöregmec 1 and Füzérkajata 2 in Hungary (Pantó 1965). The mutual contact between the high-grade and low-grade crystalline complexes was interpreted by Pantó (1965) as a remnant of the Variscan nappe structure, which means a south-verging overthrust of the high-grade crystalline rock

complex onto the low-grade metamorphic rocks. However, different opinions were expressed by Kisházi & Ivancsics (1988), who considered these low-grade metamorphic rocks as a cataclastic retrograde change of high-grade metamorphic rocks (phyllonites). The interpretation by Pantó (1965) is supported by the existence of phyllite and metarhyolite pebbles inside the overlapping Carboniferous conglomerates (Vozárová 1989). However, it should also be emphasized that manifestations of mylonitization have been found in both boreholes and surface occurrences. The Cretaceous K/Ar age of 105±4.2 and 126.6±5.2 Ma was obtained on altered plagioclase and white mica from strongly mylonitized amphibolites (Faryad & Balogh 2002). It should be mentioned that blastomylonite pebbles were found inside the Zemplinic Pennsylvanian–Permian cover conglomerates, which indicates intensive pre-Alpine ductile cataclastic deformation (Grecula & Együd 1982; Vozárová & Vozár 1988).

As for the age of the Zemplinic crystalline basement rocks, the first whole rock and muscovite Rb/Sr data from kyanite-bearing paragneisses have been interpreted as Precambrian (984±108 and 962±39 Ma; Pantó et al. 1967). Later, the K/Ar ages of amphiboles from amphibolites yielded 307 Ma, which was understood as the age of Late Variscan overprint (Lelkes-Felvári et al. 1996). A similar age of 308±12 Ma was obtained by K/Ar and $^{40}Ar/^{39}Ar$ methods in pegmatites that cut across the basement crystalline rock complex (Faryad & Balogh 2002). The Variscan age of regional metamorphism was expected based on 338±22 Ma microprobe monazite age data from paragneisses (Finger & Faryad 1999), as well as for the 338±13 and 313±13 Ma K/Ar ages of amphiboles from amphibolites (Faryad & Balogh 2002).

The Rb/Sr ages of metamorphism of the low-grade metamorphic rocks from the Hungarian territory were interpreted by Pantó et al. (1967) as Caledonian (394±52 from muscovite and 450±130 Ma from whole-rock of phyllite). However, due to their high standard deviation, these data remain questionable.

The estimated temperature and pressure conditions, which were calculated on different mineral assemblages and mineral geothermobarometer for the whole complex of rocks, varied between 600–700 °C at 550–850 MPa (Faryad 1995; Faryad & Vozárová 1997). Metamorphic pressure-temperature conditions for garnet-bearing amphibolite, estimated by these authors using the Grt–Hbl geothermometer and Grt–Hbl–Pl–Qz geobarometer, gave temperatures of 680–650 °C (core→rim) with corresponding pressures at 800–760 MPa (mineral abbreviations according to Warr 2021).

Blastomylonites were detected in the BB-1 borehole in the underlier of Neogene sediments. In the continuation of the borehole profile, a complex of variegated biotite paragneisses (with occasionally garnet and sillimanite), amphibolites, and migmatites was recognized.

More pronounced amphibolite occurrences, which are the subject of this article, come from nine horizons in the borehole (Fig. 1C).

Analytical methods

Nine samples were taken from the borehole BB-1 for petrological and geochemical studies. The location of the borehole is about 3 km southeast of the village of Byšta (GPS coordinates: 48.516702°N, 21.566015°E).

Minerals were analysed using electron microprobe JEOL JXA 8530FE at the Earth Sciences Institute in Banská Bystrica under the following conditions: accelerating voltage 15 kV, probe current 20 nA, beam diameter 3–8 μm, ZAF correction, counting time 10 s on peak, 5 s in the background. The used standards, X-ray lines and D.L. (in ppm), were: Ca (Kα, 25) – diopside, K (Kα, 44) – orthoclase, P (Kα, 41) – apatite, F (Kα, 167) – fluorite, Na (Kα, 43) – albite, Mg (Kα, 41) – diopside, Al (Kα, 42) – albite, Si (Kα, 63) – quartz, Ba (Lα, 72) – barite, Fe (Kα, 52) – hematite, Cr (Kα, 113) – Cr_2O_3, Mn (Kα, 59) – rhodonite, Ti (Kα, 130) – rutile, Cl (Kα, 12) – tugtupite, Sr (Lα, 71) – celestite.

The whole-rock chemical composition was determined at the Bureau Veritas Commodities Canada Ltd. (former ACME Analytical Laboratories Ltd., Canada). Total abundances of major element oxides were determined by inductively-coupled plasma emission spectrometry (ICP-ES) following lithium metaborate–tetraborate fusion and dilute nitric acid treatment. Concentrations of trace elements and rare earth elements were determined by ICP mass spectrometry (ICP-MS). Loss on ignition (LOI) was calculated from the difference in weight after ignition to 1000 °C. Further details are accessible on the web page of the Bureau Veritas Commodities Canada Ltd. (former ACME Analytical Laboratories; http://acmelab.com/).

To estimate the metamorphic P–T conditions, we used geothermobarometry methods and constructed phase diagrams for the studied metabasic rocks. Titanium-in-amphibole thermometry from Liao et al. (2021), Plagioclase/Amphibole thermometry from Holland & Blundy (1994), and the barometry from Molina et al. (2015) (based on Al–Si partitioning) were used with the following uncertainties: ±35 °C, ±40 °C and ±0.15–0.23 kbar expressed at 1σ. Additionally, for garnet-bearing amphibolites (484.9 m), phase equilibrium models were performed using GeoPS 2.10 (Xiang & Connolly 2022) and the internally consistent thermodynamic data set from Holland & Powell (2011, ds63) for metabasic rocks. Modelling was performed in the 11-component system MnO – Na_2O – CaO – K_2O – FeO – MgO – Al_2O_3 – SiO_2 – H_2O – TiO_2 – O_2 (MnNCKFMASHTO) using the solid-solution models by Green et al. (2016) and White et al. (2001, 2007, 2014). Solid-solution models were used as follows: cAmp(G), Gt(W), Chl(W), Mica(W), Ep(HP11), Ilm(W), Fsp(HGP) and melt(G). A value of $XFe^{3+}[=Fe^{3+}/(Fe^{3+}Fe^{2+})]=0.1$ was obtained according to the satisfactory phase modelling reproduction of the mineral assemblage and whole-rock compositions. CaO was reduced according to whole-rock phosphorous content, assuming these elements are bound exclusively to ideally composed apatite. H_2O contents were set to 5 wt% to allow free hydrous fluid phase formation at relatively low P–T. Uncertainties in the absolute location of the assemblage field

boundaries in any of the phase diagrams are estimated to be ±0.1 GPa and ±50 °C (Powell & Holland 2008; Palin et al. 2016).

Results

Petrology and mineralogy

Metabasic rocks from the BB-1 borehole are represented by typical amphibolites, which are dark-coloured with a strong to weakly foliated or lineated structure. Although their main mineral components are amphibole and plagioclase in all samples, based on their mutual content, three groups of amphibolites were defined. The apparent quartz, titanite, ilmenite, rutile, and apatite are accessories. The reaction rim of titanite around ilmenite grains occur in a direct association with plagioclase and amphibole in some places. This represents a sign of variable oxygen fugacity or H_2O activity during metamorphism (e.g., Xirouchakis & Lindsley 1998; Harlov et al. 2006; René 2008).

The ***Group-I*** amphibolites (***Grp-I***) contain around 50 % amphiboles that are arranged into dark bands alternating with bright bands of plagioclases (Fig. 2A, B). They were found at the depths of 320.6 m, 344.0 m, and 411.9 m (Fig. 1C). Typical banded gneissic structure is highlighted with alternating stripes of nematoblastic and nemato-granoblastic texture. The equilibrium mineral assemblage is Amp+Pl±Bt.

Based on their chemical composition, the amphiboles of the ***Grp-I*** amphibolites belong to calcium group with tschermakite and Mg–Fe-hornblende arrangement (according to Hawthorne et al. 2012) (Fig. 3; Suppl. Table S1). Amphiboles usually contain titanite and plagioclase, as well as ilmenite and Ti-magnetite inclusions. The Mg-hornblende and tschermakite (at the depths of 320.6 and 344.0 m) are characterised by relatively high contents of Al_2O_3 (~13–15 wt%) combined with low contents of TiO_2 (0.4–0.5 wt%), with *Mg#* values [=Mg/(Mg+Fe^{2+})] varying from 0.62 to 0.73. The composition of the Fe-hornblende (depth 411.9 m) is relatively more variable in the content of Al_2O_3 (~11–14 wt %), combined with a variable TiO_2 (0.4–1.2 wt %) with *Mg#* values varying from 0.40 to 0.50. The simple substitution Mg↔Fe is of prime importance within these studied amphiboles. The main difference between them is the relatively higher content of (Na+K) in the *A* site (0.31–0.44 *a.p.f.u.*), which corresponds to higher Fe. Composition of the associated plagioclases has a slight variation in Ca content (Fig. 3; Suppl. Table S2), corresponding to andesine in the range of An_{34}–An_{47}. They are usually uneven and secondary altered (saussuritization, sericitization, albitization). The crystals of secondary polycrystalline quartz are also found in the granoblastic aggregate along with them. Biotite, which is rarely present, is well-preserved only in the sample from the depth of 411.9 m. It is in equilibrium with amphibole and plagioclase (Fig. 2A, B). The chemical composition of biotite is linked to annite (according to Tischendorf et al. 2007; Fig. 4; Suppl. Table S3). This biotite is characterised by the TiO_2 contents in the range of 2.95–3.22 wt% and *Mg#* values of 0.38–0.40. The Na_2O and K_2O concentrations are 0.08–0.11 wt% and 9.5–9.75 wt%, respectively, suggesting only minor alterations (Suppl. Table S3).

In the ***Group-II*** (***Grp-II***) amphibolites, the equilibrium mineral assemblage is formed by amphibole (ca. 60–90 %) and plagioclase (ca. 10–40 %) samples from the depths 484.9 m, 490.8 m, and 595.9 m, which are sporadically associated with garnet (in a depth 484.9 m) and clinopyroxene (in a depth 595.9 m). Amphibole crystals frequently contain titanite, plagioclase, ilmenite, and Ti-magnetite inclusions. Based on the amphibole chemical composition, ferro-tschermakite and Fe-hornblende, with rare Mg-hornblende in the samples from the depths of 484.9 m and 490.8 m or potassic pargasite and Mg-hornblende in the sample from the depth of 595.9 m are the dominant varieties (after Hawthorne et al. 2012). They are variable in Si=6.1–6.5 and are relatively more variable in Al=1.67–2.71 *a.p.f.u.* combined with a higher Ti (0.04–0.13 *a.p.f.u.*). The *Mg#* values slightly rise with the depth of the borehole. At the depth of 484.9 m, they vary from 0.34–0.47; at 490.8 m, they correspond to 0.48–0.50; and finally, at 595.9 m, they are in the range of 0.49 to 0.58 (Fig. 3; Suppl. Table S1). The main difference is the relatively higher addition of (Na+K) in the *A* site (0.50–0.53 *a.p.f.u.*) in potassic pargasite. The chemical composition of associated plagioclases corresponds to andesine with $An_{29–37}$ and $An_{41–46}$ at the depths of 484.9 m and 490.8 m, respectively (Fig. 3; Suppl. Table S2). The composition of plagioclases is slightly different in the sample from the depth of 595.5 m, which corresponds to oligoclase with $An_{17–28}$. The brown biotite is present only at the depth of 484.9 m. It is partially chloritized in other samples. Compositions of biotite are characterised by the relatively high TiO_2 contents of 1.97–2.98 wt% and *Mg#* values of 0.27–0.46 that are linked to annite (after Tischendorf et al. 2007; Fig. 4; Suppl. Table S3). The (Na+K) *a.p.f.u.* ranges from 0.95 to 0.97, suggesting only minor alterations of these analysed crystals. Garnets belong to rare rock-forming minerals in the ***Grp-II*** amphibolites. They only occur in the sample from the depth of 484.9 m (Fig. 2C, D). Here, amphibolite is characterised by an andesine and Hbl+Grt±Bt metamorphic assemblage. Garnet encloses minor hornblende, quartz, ilmenite, and rare, biotite inclusions. It has a homogenous chemical composition without any sign of core-rim zonality. The inclusions are characterised by a relatively high content of Fe and Ca, with $Alm_{64–71}$ $Grs_{20–30}$ $Prp_{7–13}$ $Sps_{2–5}$ $Adr_{0–2}$ mol% (from 13 analyses) (Fig. 4; Suppl. Table S4). Another variability in the composition of ***Grp-II*** amphibolites is the occurrence of clinopyroxene in the sample from the depth of 595.9 m (Fig. 2E, F). This amphibolite lacks garnet with a typical metamorphic mineral assemblage: Hbl+Pl+Cpx. Clinopyroxene contains inclusions of plagioclase, amphibole, titanite, and ilmenite. Based on its chemical composition, it belongs to the group of "quadrilateral" Ca–Mg–Fe pyroxenes (diopside, according to Morimoto et al. 1988), with $Wo_{48–49}$, $En_{34–37}$, $Fs_{14–18}$ mol% (Fig. 4; Suppl. Table S5). Its *Mg#* values show relatively small variability, ranging from 0.66 to 0.73.

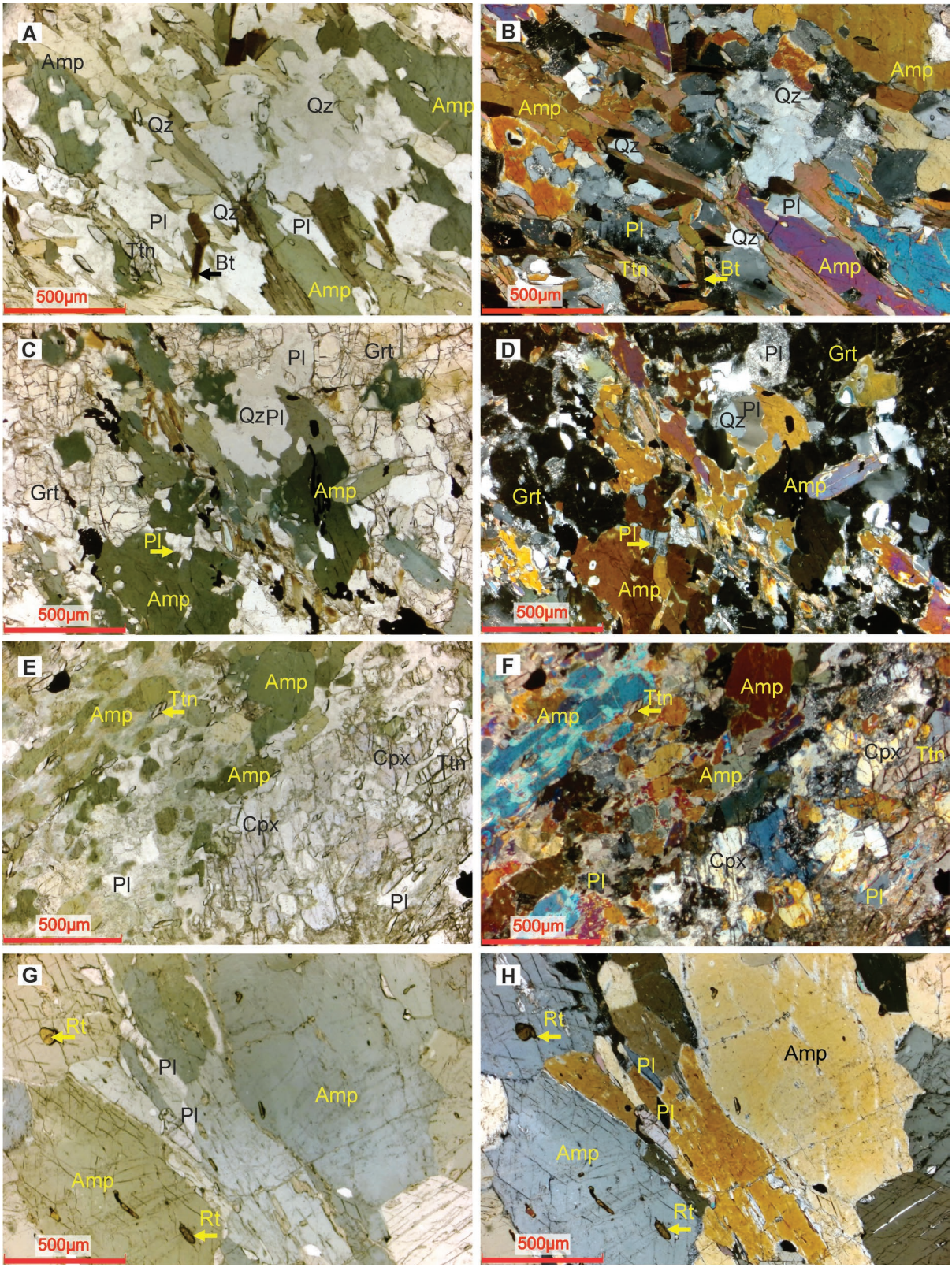

Fig. 2. Thin section images of the Zemplinic Unit amphibolite textures. **A** — Amp+Pl±Bt mineral assemblage in ***Grp-I*** amphibolites (plane-polarised light) (depth 411.9 m); **B** — the same in crossed-polarised light; **C** — Amp+Grt+Pl mineral assemblage in ***Grp-II*** amphibolites (plane-polarised light) (depth 484.9 m); **D** — the same in crossed-polarised light; **E** — Amp+Cpx+Pl mineral assemblage in ***Grp-II*** amphibolites (plane-polarised light) (depth 595.9 m); **F** — the same in crossed-polarised light; **G** — Amp+Pl mineral association in ***Grp-III*** amphibolites (plane-polarised light) **H** — the same in crossed-polarised light (depth 627.4 m). Mineral abbreviations are according to Warr (2021).

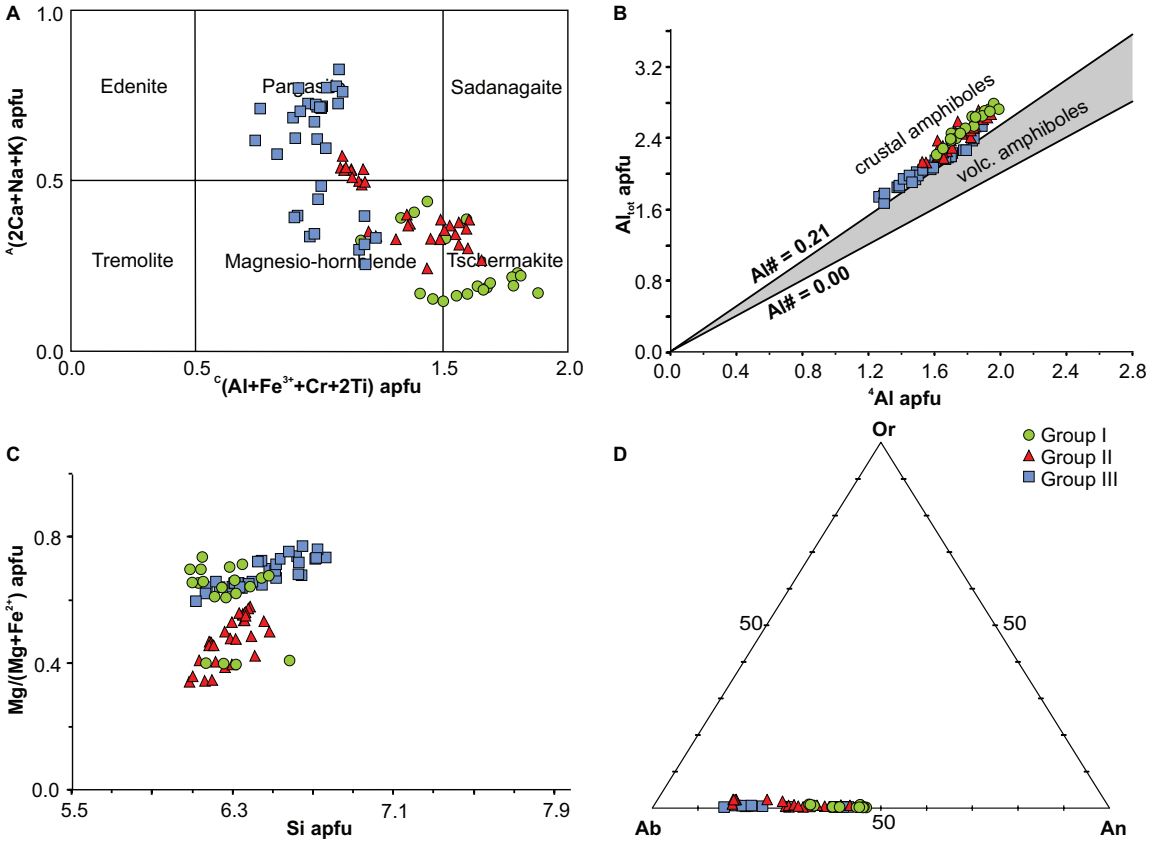

Fig. 3. Classification diagram of amphiboles and plagioclases: **A** — calcium amphiboles and their compositional boundaries according to Hawthorne et al. (2012); **B** — Al_T vs. $^{[4]}Al$ diagram for amphiboles (from Ridolfi et al. 2010) indicating their crustal origin; **C** — variation of Mg+Fe divalent cautions vs Si in the studied amphiboles; **D** — illustration of solid solutions in the plagioclases.

In addition to titanite, but not to ilmenite, the mineral assemblage with clinopyroxene contains magnetite, which means that it is more oxidized than the other two groups of amphibolites (Harlov et al. 2006).

The ***Group III*** (***Grp-III***) amphibolite with amphibole contents >95 % are unique due to the dominant presence of amphiboles in the nematoblastic texture (Fig. 2G,H). These rocks are found in the deepest levels of the BB-1 borehole and are documented with samples from a depth of 599.0 m, 613.4 m, and 627.4 m. Amphiboles from the ***Grp-III*** amphibolites correspond to the calcium amphibole group with compositions ranging from Mg-hornblende to dominant pargasite (after Hawthorne et al. 2012; Fig. 3; Suppl. Table S1). Compared to the first two groups, the ***Grp-III*** amphiboles have more variability in Al_2O_3 contents (10–14 wt%) with moderate TiO_2 (0.44–1.02 wt%). The *Mg #* values exhibit relatively low variability, both in pargasite and Mg-hornblende, with 0.59–0.77 values. However, these amphiboles differ significantly in *A* site (Na+K), which varies in the range of 0.25–0.48 *a.p.f.u.* in Mg-hornblendes, and 0.61–0.82 *a.p.f.u.* in pargasites. The composition of associated plagioclases, which form only small grains in interstitial sites, varies correspondingly. In the sample from the depth of 613.4 m, the composition is linked to the andesine with $An_{30–43}$, while at the other depths (599.0 m and 627.4 m) corresponds to oligoclase with $An_{17–24}$ (Fig. 3; Suppl. Table S2). Biotite is scarce and occurs along with amphiboles. It is heavily chloritized. This is why the chemical composition of the biotite was studied only in the sample from the depth of 627.4 m. According to Tischendorf et al. (2007), classification belongs to phlogopite (Fig. 4; Suppl. Table S3), with *Mg#* ranging from 0.67 to 0.70 and higher TiO_2 (2.14–2.58 wt%).

In the rocks studied, the amphiboles generally belong to the weak minerals or to those without secondary altered rock-forming minerals. The low-temperature secondary mineral association, which is characterised by the Chl+Act/Tr+Alb ±Ep±Cal, also appears in the entire studied group of amphibolites (albeit in small amounts). These secondary mineral associations are related to the hydration of amphibolites during the retrograde re-equilibration of the whole complex.

The composition of the studied amphiboles expressed by the aluminium number ($Al\# = {}^{[6]}Al/Al_{Tot}$) is consistent with a field of crustal amphiboles, since they were earmarked according to Ridolfi et al. (2010) for crustal and experimental calcium amphiboles. In comparison to the $Al_{Tot}/{}^{[4]}Al$ diagram (Ridolfi et al. 2010), amphiboles from the BB-1 amphibolites are identical to metamorphic, crustal amphiboles. Figure 3B shows that the analysed amphiboles are concentrated in a relatively

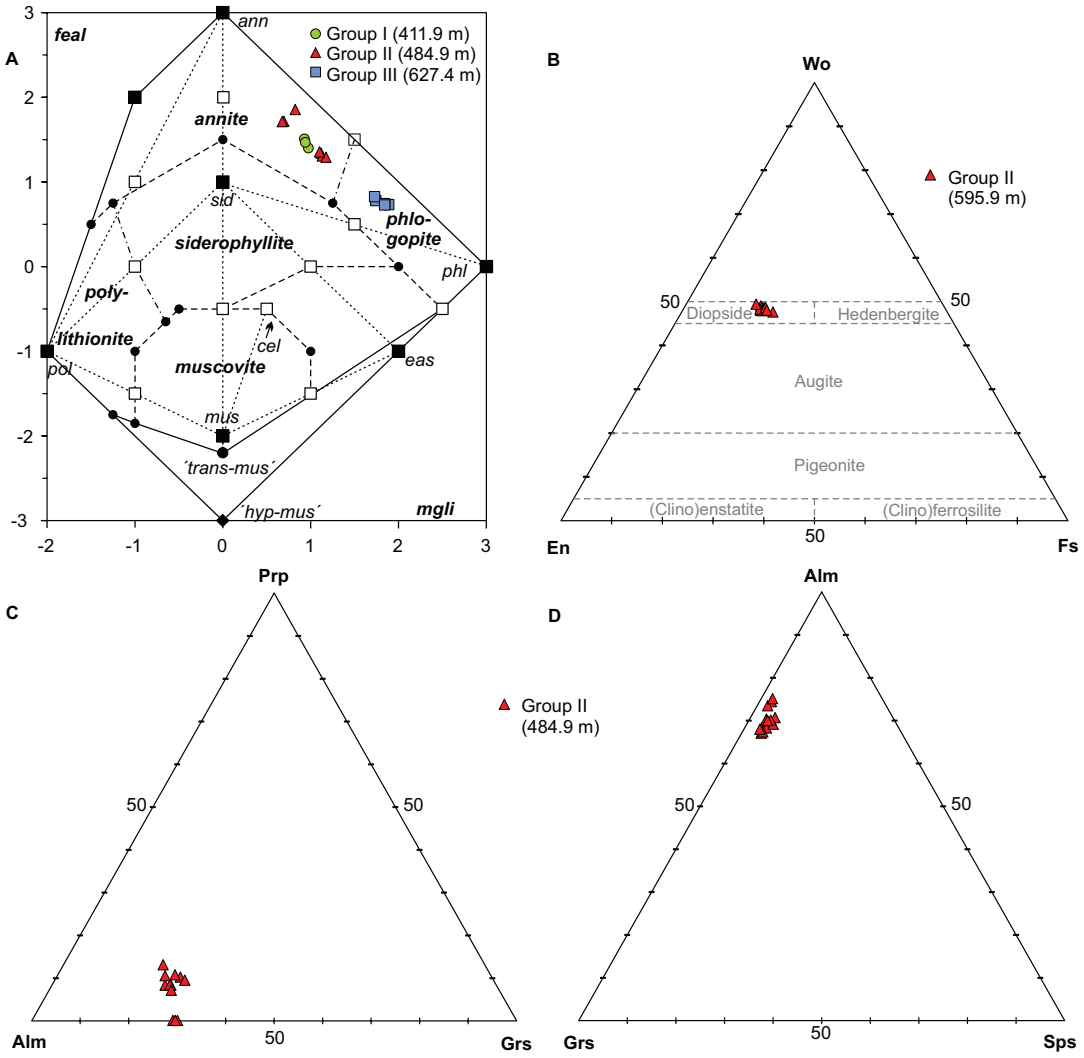

Fig. 4. Classification diagrams of remaining rock-forming minerals: **A** — biotites (from Tischendorf et al. 2007); **B** — clinopyroxenes (from Morimoto et al. 1988); **C, D** — end-member molecules in the garnets.

homogeneous field. However, minor differences can be distinguished. While Mg-hornblende and tschermakite subgroups have Al# values (hereafter referred to as the aluminium number, i.e., $^{[6]}Al/Al_T$, calculated on the basis of Ridolfi et al. 2010) in the range of 0.24–0.32, Al# values are generally lower in the potassic pargasite and pargasite subgroup, ranging from 0.20–0.25.

Metamorphic constraints

Previous petrological analyses pointed out that the Zemplinic crystalline basement rocks were regionally metamorphosed under amphibolite facies conditions. To verify this metamorphic data, a new set of chemical compositions of mineral phases were used. Titanium-in-amphibole thermometry according to Liao et al. (2021) and the Plagioclase/Amphibole barometry of Molina et al. (2015) based on Al–Si partitioning were used with the following uncertainties: ±35 °C, ±0.15–0.23 GPa expressed at 1σ.

All P–T estimates of the studied samples fall within the P–T interval of the amphibolite facies with conditions of 545–735 °C at 0.41–0.88 GPa (Fig. 5) based on Ti-in-Amp thermometry. Only negligible differences were found within the individual amphibolite groups. The ***Grp-I*** of amphibolites (320.6 m, 344.0 m and 411.9 m) show the lowest temperatures between 550–615 °C (mean 585 °C) at moderate pressures of 0.49–0.70 GPa (mean 0.63 GPa). The amphibolite sample from 411.9 m (with present Bt) reaches up to 735 °C (mean 655 °C) at higher pressure 0.71–0.85 GPa (mean 0.75 GPa). The ***Grp-II*** of amphibolites spans a similar P–T interval of 560–725 °C (mean 665 °C) at 0.67–0.88 GPa (mean 0.79 GPa). Within the group, the Cpx-bearing amphibolites (595.9 m) show the highest temperatures between 660–725 °C (mean 690 °C) and pressures between 0.78–0.88 GPa (mean 0.84 GPa). Grt-bearing samples (484.9 m) span the interval of 615–710 °C (mean 660 °C) at 0.72–0.83 GPa (mean 0.76 GPa). The ***Grp-III*** amphibolites show conditions of 570–700 °C (mean 650 °C) at 0.41–0.78 GPa (mean 0.63 GPa). Amp–Pl

thermometry (Holland & Blundy 1994) temperature estimates show the interval of 570–720 °C for the studied samples (Suppl. Table S1). These values are within the given uncertainties with Ti-in-Amp thermometry.

Phase equilibrium modelling was used to estimate P–T conditions for the metamorphic assemblage (Amp+Grt+Pl+Ilm +Ttn+Qz) of garnet-bearing samples in ***Group-II*** amphibolites (at the depth of 484.9 m) of the Zemplinic crystalline basement (Fig. 6). Isopleths geo-thermo-barometry show P–T values of 570–670 °C at 0.60–0.80 GPa using the following isopleths of a sample composition: $Prp_{0.07–0.13}$, $Grs_{0.20–0.27}$ and Ti-in-Amp $_{0.06–0.12}$ (Suppl. Tables S1, S4). These estimates correspond with the results obtained by Ti-in-Amp thermometry and Amp–Pl geobarometry within the given uncertainties.

Geochemistry

The major and trace element compositions of the BB-1 boreholes metabasites are given in Table 1.

The SiO_2 concentrations generally range between 38 and 53 wt%, typical of basaltic composition. However, these contents can be partly affected by rarely present xenomorphic crystals of a secondary quartz in texture (Fig. 2A, B). The large range of MgO (4.02–13.24 wt%), which is coupled with variable Ni contents (27–380 ppm), indicates that all amphibolites are derived from differentiated magma. This is also illustrated in extremely variable *Mg#* values ranging between 0.41 and 0.77.

However, all samples are amphibolites and it is therefore likely that alkali metals, as well as other large ion lithophile elements (LILE; Cs, Rb, Ba, Pb and Sr), were affected to some degree by either hydrothermal and/or regional metamorphism (e.g., Pearce 1976; MacGeehan & MacLean 1980; Rollinson 1993). Therefore, we mainly rely on trace elements in the following classification and discussion, which are considered to be less mobile during alteration and metamorphism (e.g., Dostal & Capedri 1979; Gelinas et al. 1982; Humphris 1984; Grauch 1989).

The compositional diversity of these rocks is conspicuous on the Zr/Ti vs Nb/Y diagram of Winchester & Floyd (1977), which was later revised by Pearce (1996) (Fig. 7A). Based on this chemical classification, the protolith amphibolites correspond to the two different volcanic groups; the first (samples from 320.6 to 484.9 m) among the sub-alkali basalt (Nb/Y= 0.05–0.31) and the second (samples from 490.8 to 627.4 m) in the alkali basalt fields (Nb/Y=0.90–1.85; Fig. 7A).

Due to the chemical composition, ***Grp-I*** amphibolite protolith coincides with sub-alkaline basalts. The ***Grp-II*** and ***Grp-III*** amphibolite protoliths closely coincide with the composition of alkaline basalts (Fig. 7A). Sample BB4 from a depth of 484.9 m is the only transient sample that shows insignificant affinity for alkaline basalts in all classification diagrams.

The studied metabasic rocks differ strongly in TiO_2 contents. The ***Grp-I*** amphibolites, with TiO_2 ranging from 0.6 to 2.1 wt% and Ti/Y ratios between 260 and 351, is placed to the low-Ti basalts. In contrast, the ***Grp-II*** and ***Grp-III*** amphibolites are characterised by a relatively higher content of TiO_2 (from 2.6 to 3.1 wt%) and Ti/Y ratios between 497 and 834, which classes them to high-Ti basalts.

The metabasic rocks are characterised by variable contents of incompatible elements (rare earth group elements – REE and high field strength elements – HFSE) exemplified by the concentration ranges of ΣREE with ***Grp-I*** amphibolites in the range of 41.6–137.8 ppm and ***Grp-II*** and ***Grp-III*** amphibolites between 137.9 and 214.7 ppm. Differences are also in Zr, 54.8–208.3 ppm in ***Grp-I*** amphibolites and 179.4–233.1 ppm in ***Grp-II*** and ***Grp-III*** amphibolites and Nb concentrations, 1.1–11.0 ppm and 29.0–47.3 ppm, respectively.

The ***Grp-I*** amphibolites show relatively flatter REE patterns (normalized according to McDonough & Sun 1995) with 7 to 80 chondritic concentrations, compared to the ***Grp-II*** and ***Grp-III*** amphibolites, which display steeper REE patterns with 10 to 175 chondritic concentrations (Fig. 7B). However, the Eu anomaly is around 1.0 in all analysed samples (Eu/Eu*= 0.89–1.04 and 0.95–1.19, respectively) and attests to some minor accumulation or fractionation of plagioclases. Both groups of metabasic rocks are characterised by highly fractionated LREE/HREE chondrite normalized patterns (Fig. 7B). The ***Grp-II*** and ***Grp-III*** amphibolites show more LREE-enrichment [$(La/Yb)_{CN}$=9.22–17.11] than ***Grp-I*** amphibolites [$(La/Yb)_{CN}$=1.50–5.89]. Moreover, $(Tb/Yb)_{CN}$ values in amphibolites with protolith derived from alkaline basalts range from 2.02 to 3.92 indicating an MREE from HREE fractionations, whereas the ***Grp-I*** amphibolites, which are derived from sub-alkaline basalts, show rather weak fractionations [$(Tb/Yb)_{CN}$=1.27–2.14)].

The presumably less mobile REE (La, Ce, Pr, Nd, Sm, Eu, Dy, Yb, Lu) plus some HFSE (Zr, Ti, Y, with Th and Nb are relatively low, some even below a detection limit (Th in the sample BB2, Ta in the samples BB1 and BB2; Table 1), especially in the ***Grp-I*** amphibolites. In contrast, the hydrous fluid elements (Cs, Rb, Ba, U, K, Pb, Sr) are enriched. The patterns of the ***Grp-II*** and ***Grp-III*** amphibolites show higher normalized trace-elements concentrations compared to the ***Grp I*** amphibolites, with the exception of the HREE, which also show depletion (Fig. 7C, D).

E-MORB (enriched-type mid-ocean ridge basalt) normalized plot (from Sun & McDonough 1989) of the ***Grp-II*** and ***Grp-III*** amphibolites display patterns transitional between E-MORB and OIB (ocean island basalt) (Fig. 7C) that are consistent with their elemental ratios; e.g., Ti/V=21–57 and 50–62, respectively; Zr/Nb=19–50 and 4.5–7.5, Zr/Y=2.3–5.8 and 6.7–9.8, Nb/Yb=0.5–4.2 and 11–28, La/Nb=1.8–4.8 and 0.7–1.2, respectively. The protolith ***Grp-I*** amphibolites, based on the content of trace elements and their distribution inclines to E-MORB basalt, with evidence of Zr–Hf, Ti, Y and Nb depletion. On the other hand, the ***Grp-II*** and ***Grp-III*** amphibolite protoliths tend to be more transitional to the OIB basalt (Fig. 7C), with evidence of higher enrichment in LREE and MREE, as well as in Th, U, and Nb (e.g., Sun & McDonough 1989; Pearce 1996, 2008). The same trends are shown in

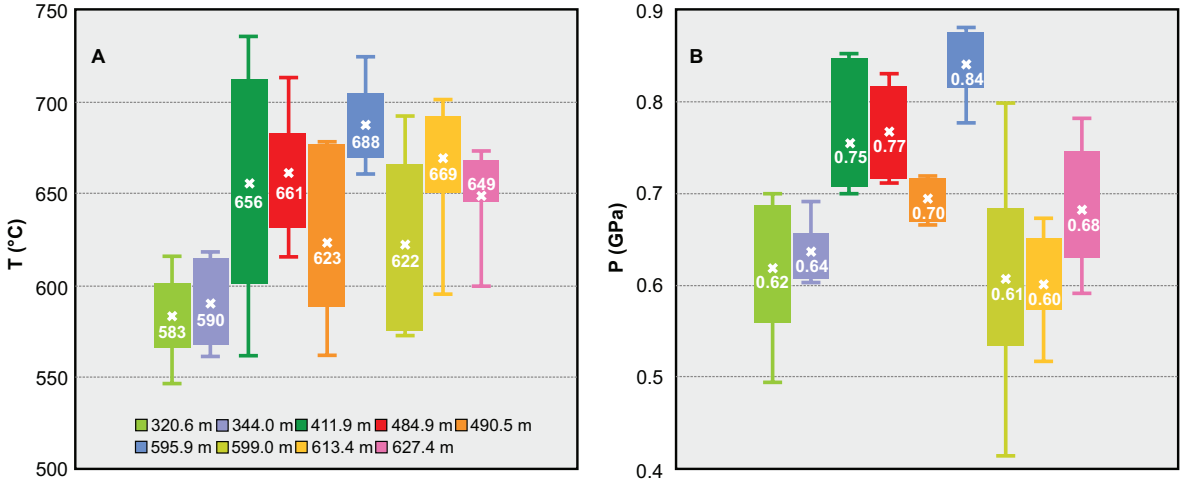

Fig. 5. P–T condition diagrams comparing all studied metabasic samples of Zemplinic crystalline basement. **A** — Temperature estimates based on Ti-in-Amp geothermometry (Liao et al. 2021); **B** — Pressure estimates based on Amp–Pl geobarometry (Molina et al. 2015). Vertical lines represent an interval of all temperatures/pressures of a sample, rectangles represent placement of the majority of calculated values within the set, crosses represent average value of a temperature/pressure.

the incompatible element's diagram normalized to N-MORB (normalizing values according to Sun & McDonough 1989) (Fig. 7D).

Discussion

P–T evolution

The studied amphibolites are characterised mainly by andesine feldspars and green/dark-green amphiboles, which are associated with Bt, Qz, Grt, and Cpx in some places. All pressure-temperature estimates of the studied samples fall within the P–T interval of the amphibolite facies with conditions between 550–725 °C at 0.4–0.83 GPa. However, some differences can be observed between the individual groups of amphibolites. The lowest temperatures (mean 585 °C) and pressures (mean 0.63 GPa) were found in the ***Grp-I*** amphibolites at the depths of 320.6 and 344.0 m (Fig. 4A, B). The relatively lower temperature part of the amphibolite facies is also evidenced by the fact that Bt+Pl±St paragneisses are associated (Vozárová 1991).

In general, the calculated temperatures in the other amphibolites (***Grp-II, Grp-III***) are approximately the same, averaging between 650 °C and 690 °C, but with greater pressure variability between 0.63 and 0.85 GPa (Fig. 5A, B). In contrast, the highest temperatures 660–725 °C and pressures 0.78–0.88 GPa, are shown in the sample from the depth of 595.9 m with the association Hbl+Pl+Cpx (Fig. 5A, B). These calculated temperatures and pressures correspond to the climax of the orogenic metamorphism of

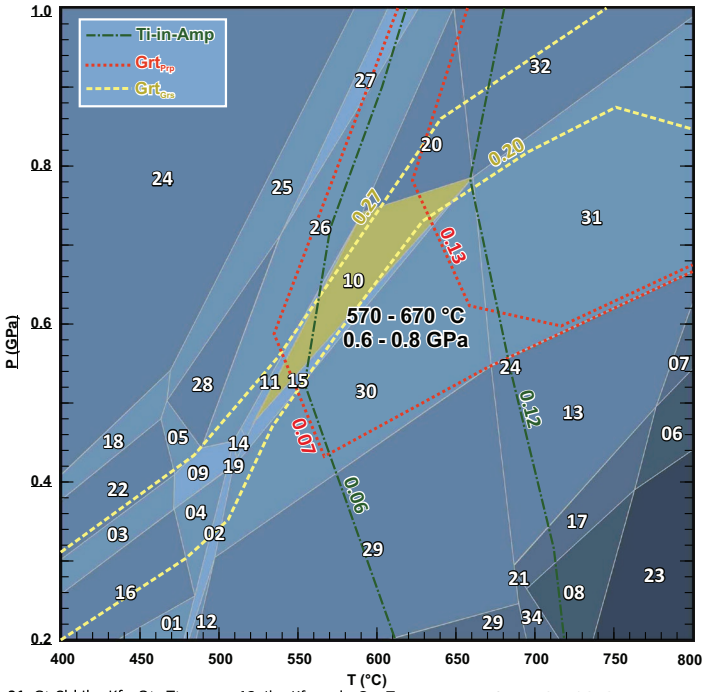

Fig. 6. P–T pseudosection calculated by GeoPS thermodynamic software (Xiang & Connolly 2021) for the metamorphic assemblage of garnet-bearing samples of a ***Group-II*** amphibolites (in a depth 484.9 m) of the Zemplinic Crystalline basement. Whole-rock composition used for modelling can be found in Table 1.

Table 1: Representative major oxides and trace elements, including REE in the Zemplinic metabasic rocks (n.d. – sample below detection limit; Ta=0.1ppm; Th=0.2 ppm).

sample		**BB1**	**BB2**	**BB3**	**BB4**	**BB5**	**BB6**	**BB7**	**BB8**	**BB9**
depth	m	320.6	344.0	411.9	484.9	490.8	595.9	599.0	613.4	627.4
SiO_2	wt%	47.47	50.03	53.29	51.82	50.86	43.86	41.91	42.73	38.08
Al_2O_3	wt%	18.70	19.83	17.62	16.96	15.52	9.52	12.19	12.14	9.36
Fe_2O_3	wt%	10.53	8.06	7.11	10.91	11.57	12.77	13.31	13.00	12.14
MgO	wt%	4.58	5.56	5.04	4.12	4.02	13.50	13.24	9.45	11.65
CaO	wt%	9.98	9.08	7.02	7.83	8.89	13.34	9.61	13.45	17.15
Na_2O	wt%	3.32	3.92	4.00	3.61	3.23	1.53	1.73	2.43	1.57
K_2O	wt%	1.50	0.51	1.46	1.20	1.27	0.67	1.76	0.98	0.74
TiO_2	wt%	1.02	0.71	0.58	2.09	2.67	2.59	2.86	3.13	2.81
P_2O_5	wt%	0.12	0.18	0.11	0.29	0.42	0.32	0.40	0.43	0.45
MnO	wt%	0.21	0.11	0.10	0.13	0.14	0.16	0.19	0.17	0.19
Cr_2O_3	wt%	0.01	0.01	0.02	0.02	0.01	0.15	0.08	0.08	0.14
Ni	ppm	33	54	61	26	27	355	215	236	380
Sc	ppm	35	25	21	30	25	35	34	28	28
LOI	wt%	2.4	1.8	3.5	0.8	1.1	1.2	2.3	1.6	5.0
sum	wt%	99.82	99.80	99.84	99.78	99.72	99.65	99.61	99.63	99.32
Ba	ppm	292	165	389	419	363	151	457	217	128
Co	ppm	31.4	28.6	21.4	34.7	34.4	67.1	53.0	57.0	66.1
Cs	ppm	2.8	4.2	9.2	1.8	1.6	0.3	2.1	1.0	0.2
Ga	ppm	19.0	24.2	22.9	27.3	24.5	17.7	22.9	20.3	16.5
Hf	ppm	1.7	1.8	2.0	5.9	6.3	5.4	5.2	6.8	5.5
Nb	ppm	1.1	2.1	2.7	11.0	29.0	30.4	43.1	47.3	36.8
Rb	ppm	46.3	17.1	64.1	33.8	31.2	8.6	40.6	15.5	10.8
Sr	ppm	351.3	818.5	554.1	320.3	726.6	155.9	213.8	463.6	214.7
Ta	ppm	n.d.	n.d.	0.5	1.1	2.2	2.0	3.1	3.2	2.6
Th	ppm	1.5	n.d.	1.3	3.0	4.3	2.3	3.9	5.2	2.8
U	ppm	0.4	0.2	0.9	1.5	1.2	0.6	1.0	1.1	0.9
V	ppm	296	186	163	220	258	308	331	320	319
Zr	ppm	54.8	59.1	55.7	208.3	215.5	179.4	195.7	233.1	200.6
Y	ppm	23.5	15.8	13.2	35.6	32.2	18.6	22.4	25.5	20.5
La	ppm	5.1	10.1	9.8	19.9	35.3	21.1	34.1	41.6	33.0
Ce	ppm	12.9	26.1	23.0	47.3	75.3	51.4	73.0	84.9	71.9
Pr	ppm	1.97	4.02	3.19	6.68	9.69	7.23	9.16	11.02	9.30
Nd	ppm	10.3	19.8	14.5	31.8	40.9	34.4	38.0	46.0	37.0
Sm	ppm	2.75	4.25	2.67	7.11	8.24	6.85	7.24	9.17	6.33
Eu	ppm	1.01	1.23	0.91	2.15	2.44	2.06	2.02	2.72	2.19
Gd	ppm	3.62	3.71	2.68	7.52	7.33	5.70	5.72	7.12	4.95
Tb	ppm	0.66	0.53	0.41	1.25	1.18	0.86	0.87	1.12	0.89
Dy	ppm	3.94	2.69	2.25	6.64	5.95	4.39	4.65	5.18	4.20
Ho	ppm	0.84	0.57	0.46	1.26	1.15	0.71	0.80	1.00	0.75
Er	ppm	2.42	1.54	1.21	3.19	2.84	1.55	1.97	2.38	1.84
Tm	ppm	0.40	0.26	0.19	0.45	0.40	0.23	0.30	0.36	0.25
Yb	ppm	2.31	1.44	1.13	2.60	2.60	1.24	1.59	1.87	1.31
Lu	ppm	0.37	0.20	0.18	0.36	0.38	0.18	0.23	0.25	0.18
C_{Tot}	%	0.28	0.15	0.45	0.07	0.08	0.20	0.07	0.56	1.36
S_{Tot}	%	0.13	0.10	0.02	0.03	0.15	0.03	0.14	0.11	0.05
Eu*		0.976	0.944	1.037	0.896	0.957	1.005	0.957	1.026	1.193
Nb/Y		0.047	0.133	0.205	0.309	0.901	1.634	1.924	1.855	1.795
Zr/Ti		0.009	0.014	0.016	0.017	0.013	0.012	0.011	0.012	0.012

the Zemplinic crystalline basement. This roughly confirms the data obtained from the associated Grt+Bt±Sill gneisses, as well as from the Grt-amphibolites calculated by Faryad (1995) and Faryad & Vozárová (1997).

According to the calculated temperatures and pressures, a substantial part of the studied amphibolites indicates P–T conditions of the upper amphibolite facies. In comparison, the calculated temperatures and pressures are lower in the samples from the upper part of the BB-1 borehole in the range of the middle part of the amphibolite facies, which could be a manifestation of retrogression changes, however, tectonic contact along a ductile shear zone is not excluded between these two complexes. This interpretation is supported by frequent occurrences of mylonite that have previously been described in the upper part of the BB-1 borehole (Vozárová 1991).

Source of mafic magma

The Zemplinic metabasic rocks are characterised by depletion in HREE with respect to MREE. In fact, the $(Sm/Yb)_{CN}$ ratios are significantly higher than those of typical N-MORB

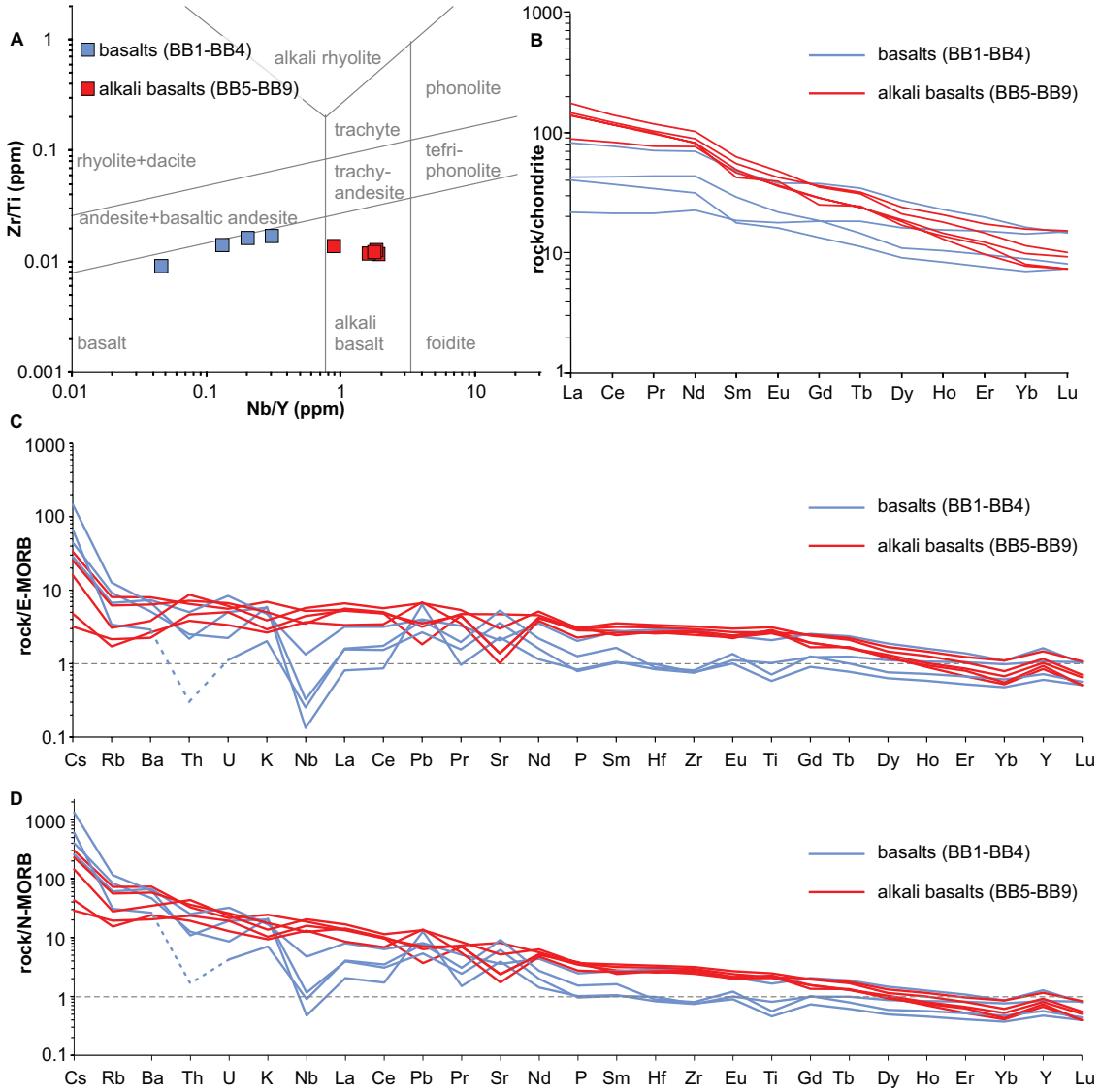

Fig. 7. A — Distribution of the Zemplinic metavolcanic rocks based on Zr/Ti versus Nb/Y according to Pearce's diagram (1996) (revised by Winchester & Floyd 1977); **B** — Chondrite normalized REE distribution of the studied samples. Chondrite normalizing values according to McDonough & Sun (1995); **C** — E-MORB normalized incompatible element's diagram of the studied samples. Normalizing values according to Sun & McDonough (1989); **D** — N-MORB normalized incompatible element's diagram of the studied samples. Normalizing values according to Sun & McDonough (1989).

$((Sm/Yb)_{CN}=0.96$, Sun & McDonough 1989), since they range from 1.29 to 2.97 for the ***Grp-I*** amphibolites and from 3.45 to 6.01 for the ***Grp-II*** and ***Grp-III*** amphibolites. Such distinctive depletion in HREE with respect to MREE in the ***Grp-II*** and ***Grp-III*** amphibolites is interpreted as a clear garnet signature in their mantle source. Montanini et al. (2008) and Saccani et al. (2008) suggested that these types of basalts originated from partial melting of a depleted mantle source characterised by garnet-bearing mafic layers.

Less HREE depleted ***Grp I*** amphibolites, with sub-alkaline metabasalt protolith, are reminiscent of continental margin MORB (Dilek & Furnes 2011) or C-MORB (Pearce 2008) characteristics, which is more likely indicative of a spinel-bearing peridotite mantle source and lacking a significant content of residual garnet during the melting event. They are commonly considered the products of low degrees of melting of less-depleted sub-continental lithospheric mantle and upwelling asthenosphere (Rampone et al. 2005). In comparison, the group of higher HREE depleted the ***Grp-II*** and ***Grp-III*** amphibolites with alkali basalt protolith corresponds mainly to OIB or P-MORB with variable garnet influence, which results in marked LILEs (large ion lithophile elements) enrichment and high LREE/HREE ratios $[(La/Yb)_{CN}=$ 9.22–17.11].

On the Th_N vs. Nb_N diagram (from Saccani 2015, based on Th–Nb proxies of Pearce 2008; N-MORB normalized according to Sun & McDonough 1989), the studied Zemplinic metabasic rocks are plotted in two different groups (Fig. 8A).

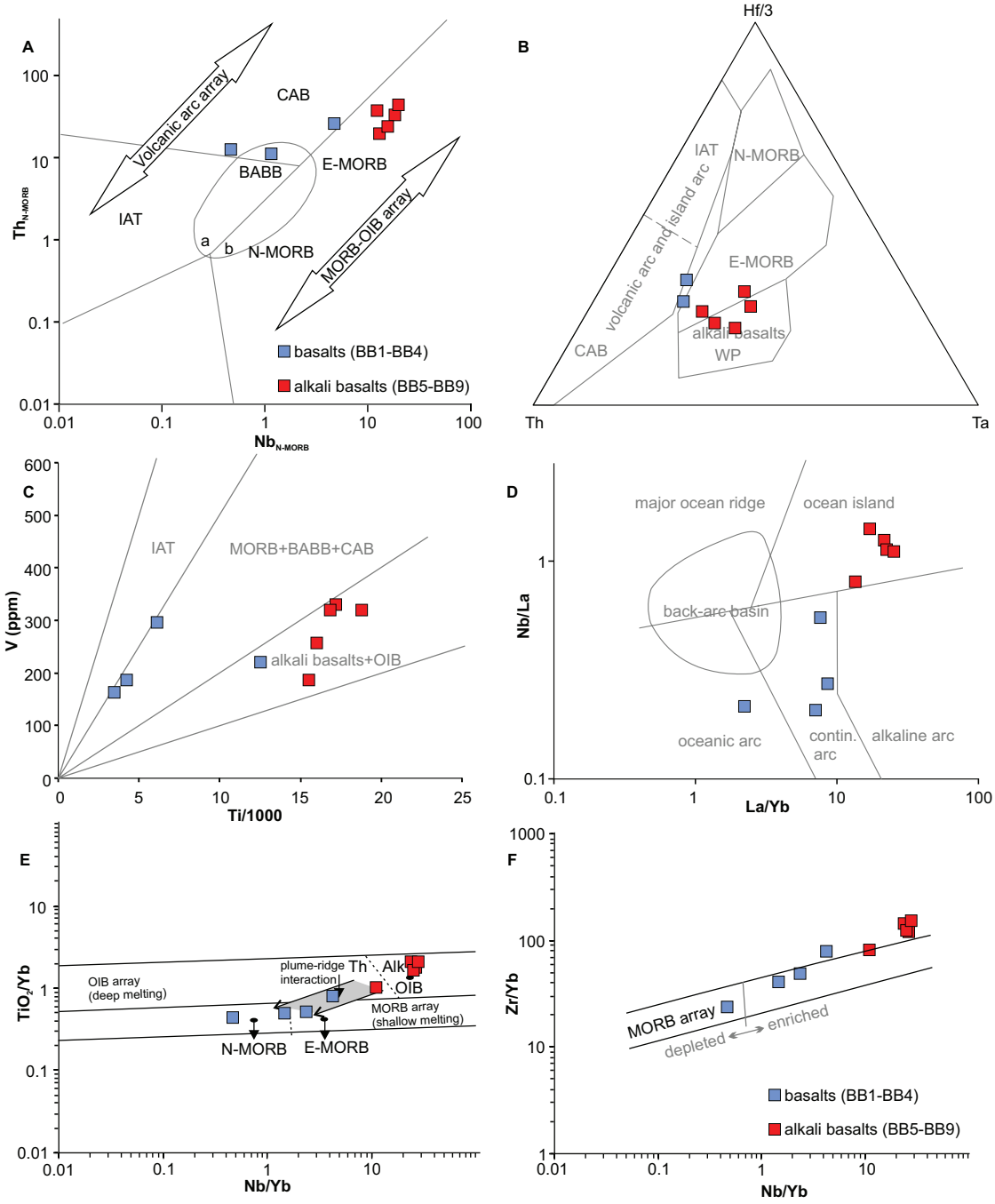

Fig. 8. Trace element discrimination diagrams for the petrogenetic and tectonic interpretation of the Zemplinic crystalline basement metabasic rocks: **A** — Tectonic interpretation of ophiolitic basalts based on $Th_{N\text{-}MORB}$–$Nb_{N\text{-}MORB}$ systematics (from Saccani 2015); **B** — Hf–Th–Ta diagram (from Wood 1980); **C** — V vs. Ti/1000 metabasalt classification (from Shervais 1982); **D** — Nb/La–La/Yb discriminant diagram (from Hollocher et al. 2012); **E** — TiO_2/Yb vs. Nb/Yb discriminant diagram distinguishing OIB and MORB arrays in the intra-oceanic basalts (from Pearce 2008); **F** — Zr/Yb vs. Nb/Yb showing depleted and enriched N-MORB trends (from Pearce & Peate 1995).

The ***Grp-I*** amphibolites with sub-alkaline metabasalt protolith correlate more to volcanic arc and island-arc tholeiites (CAB, IAT) or back-arc basin basalt (BABB) fields. The ***Grp-II*** and ***Grp-III*** amphibolites with alkali metabasalt protolith correspond to E-MORB and partially overlap with P-MORB or alkali basalts (AB). Wood's (1980) and Shervais's (1982) classical discrimination diagrams show a very similar distribution (Fig. 8B, C). It is interpreted as CAB and IAT for the ***Grp-I*** amphibolites and OIB and WP for the ***Grp-II*** and ***Grp-III*** amphibolites. Based on the relationship Nb/La vs. La/Yb (after Hollocher et al. 2012), the studied ***Grp-I*** amphibolites are plotted between LREE-enriched ocean island and arc component arrows (Fig. 8D). Moreover, based on the Nb_N/La_N ratios (N-MORB normalized according to Sun & McDonough

1989), the studied metabasic rocks belong to different groups with LREE enriched values of 0.88–1.55 (***Grp-II*** and ***III*** amphibolites) and LREE depleted values of 0.22–0.59 (***Grp-I*** amphibolites). In both groups of these metabasic rocks, there is also wide variability in La contents, ranging from 21 to 41 ppm and from 5 to 19 ppm, respectively. These values reflect the difference between MORB- and ocean island-type magma sources (Sun & McDonough 1989; Nb_N/La_N ratios ~1), as well as the magma source regions of volcanic arcs (Nb_N/La_N ratios <1; e.g., Pearce & Peate 1995; John et al. 2004; Pearce & Stern 2006; Hollocher et al. 2012). Arc volcanics can be thought of as being derived from a depleted MORB-like mantle that has been variably enriched with subduction zone components (e.g., Pearce & Stern 2006; Dilek et al. 2007; Martinez et al. 2007; Ilnicki et al. 2020; Altherr et al. 2021). In fact, the Zemplinic metabasic rocks have negative Nb anomalies and either none or slight Zr–Hf and Ti anomalies.

In the Nb/Yb–Ti/Yb diagram (from Pearce 2008), the ***Grp-I*** amphibolite projection points are plotted in the MORB array, and conversely in the ***Grp-II*** and ***Grp-III*** in the OIB array (Figs. 8E). The difference between MORB and OIB reflects the fact that OIB, located on thick lithosphere, have garnet residues, whereas MORB, located on thin lithosphere, do not (Pearce 2008). Similarly, in the Zr/Yb vs. Nb/Yb diagram (Fig. 8F), projection points the half part of the studied samples plot within the MORB array and others plot toward high Zr/Yb ratios of the OIB array. The concentration of the subduction-mobile elements (Th, La, and K) relative to the more subduction-immobile elements (Nb and Ta) gives the negative Nb anomaly diagnostic of arc volcanism in geochemical patterns (e.g., Pearce & Peate 1995; Pearce 1996; Turner et al. 2014). The Th/Yb ratio values of the Zemplinic metabasic rocks are variable and relatively high (from 0.65 to 1.15 for the ***Grp-I*** amphibolites; from 1.15 to 2.78 for ***Grp-II*** and ***Grp-III*** amphibolites), which might indicate contamination by continental crust or through interaction with the sub-continental lithospheric mantle (Pearce 2014). Similarly, based on Zr/Nb and Nb/Th ratios, the Zemplinic metabasic rocks defined two distinct populations: the ***Grp-I*** amphibolites form an assemblage with Zr/Nb ratios ranging from 19 to 50 and Nb/Th ratios ranging from 0.7 to 4; in comparison, the ***Grp-II*** and ***Grp-III*** amphibolites have low Zr/Nb ratios ranging from 4.5 to 7.5 and higher Nb/Th ratios from 7 to 13. According to Condie (2003), the high Zr/Nb ratios and also the low Nb/Th ratios shifted the Zemplinic ***Grp-I*** amphibolites to hypothetically enriched mantle sources. In comparison, the Zemplinic ***Grp-II*** and ***Grp-III*** amphibolites with the low Zr/Nb ratios and the higher Nb/Th ratios correspond with plume-related OIB source, having recycled components in its mantle. It is assumed to be representative of recycled oceanic lithosphere (Saunders et al. 1988; Hofmann 1997; Condie 2003).

Rudnick (1995) and Condie (1999) used a La/Nb ratio of 1.4 to distinguish basalts erupted on ocean ridges, islands, and plateaus from those erupted in arcs. The ***Grp-I*** amphibolites, with La/Nb ratio values in the range of 1.8–4.8, indicate basalt protolith containing a subduction component and/or contamination by continental crust. On the contrary, the ***Grp-II*** and ***Grp-III*** amphibolites, with low La/Nb ratio values in the range of 0.7–1.2, indicate an oceanic source corresponding to OIB protolith.

The metasomatic enrichment in the ***Grp-I*** amphibolites was induced by fluid-related subduction metasomatism because the lower values of Th/Nd (<0.15) indicate hydrous fluids released from the slab (Woelki et al. 2018).

Geodynamic implication

Geochronological data on the age of the Zemplinic crystalline basement confirm a Neoproterozoic–Early Paleozoic age of its protolith. At the same time, however, they do not exclude an Early Paleozoic age of its metamorphism, partially rejuvenated in the Variscan and Alpine orogens (Pantó et al. 1967; Lelkes-Felvári et al. 1996; Finger & Faryad 1999; Faryad & Balogh 2002). This hypothesis is indirectly confirmed by the results of U–Pb (SHRIMP) dating of detrital zircons, which were obtained from the Zemplinic Pennsylvanian–Permian envelope sedimentary sequence (Vozárová et al. 2019a). The summary of the zircon age data was as follows: Ordovician 40 %, Cambrian 2 %, Ediacaran–Cryogenian 37 %, Tonian 5 %, Stenian–Ectasian 2 % and Paleoproterozoic–Neoarchean 13 % (from 134 grains in total with >95 % concordance) (Vozárová et al. 2019a). Of the entire number of analysed detrital grains, only one zircon grain was found with a concordant age of 355±5 Ma and only in the youngest, Permian sediments of the Late Paleozoic part of the envelope. The other two inherited grains, aged 347±5 and 348±5 Ma, were found in Pennsylvanian pyroclastic rocks that are a part of an envelope sequence. Largely, the whole set of the analysed detrital zircons, when taking into consideration the $^{232}Th/^{238}U$ values and their internal textures, determined a felsic magmatic origin (Vozárová et al. 2019a). The Ediacaran–Cryogenian peak ages at 592 Ma and 641 Ma, as well as smaller peaks between ~773 to 950 Ma evidently document Pan-African multiple magmatic events (a chronologic equivalent of the Cadomian Orogeny in Western and Central Europe), which are currently interpreted resulting from amalgamation of juvenile and continental arc domains during the period ~870 to ~550 Ma in the peri-Gondwanan realm (e.g., Murphy & Nance 1989; Nance et al. 2002; Kröner & Stern 2004; Linnemann et al. 2008; Stampfli et al. 2013; Gärtner et al. 2013; Henderson et al. 2016 and references therein). Herewith, the acquired zircon spectra indicate that the Cadomian arc magmatism was contaminated with variable amounts of Eburnian and Neoarchean crust. However, the largest group among detrital zircon spectra is represented by the Middle/Upper Ordovician assemblages. These indicate widespread magmatic activity at 444–476 Ma, which was likely connected with the beginning of a massive extension and opening of the eastern Rheic Ocean, followed by drifting of the Gondwanan ribbon-microcontinents (Stampfli et al. 2013 with references therein). At this stage, voluminous calc-alkaline and peraluminous volcanic rocks were produced (e.g.,

Neubauer 2002 – the Middle Austroalpine basement; Roger et al. 2004 – the French Central Massive; Putiš et al. 2008 – the Western Carpathians; Balintoni et al. 2009 – Romanian Carpathians; Vozárová et al. 2010, 2017 – the Western Carpathians; Casas et al. 2010 – the Pyrenees; von Raumer et al. 2013 – the Alps; Bonev et al. 2013 – Rhodope Massif; Dörr et al. 2015 – External Hellenides; Antić et al. 2016 – the Serbo–Macedonian Massif; Sirevaag et al. 2016 – the Elba Island).

It follows that the Zemplinic Neoproterozoic arc crust had been affected by the extensional thermal relaxation and melting during the Middle/Late Ordovician. The presence of the Neoproterozoic detrital zircon ages, including the Tonian ones, allow for comparison of the Zemplinic basement source area with the eastern peri-Gondwanan domain, which was situated at the northern margin of the Saharan Metacraton or the Arabian Nubian Shield (Vozárová et al. 2019a). According to the results of Stephan et al. (2019), the Ordovician calc-alkaline and peraluminous magmatism predominated in the East African–Arabian Zircon Province with two main pulses at ca. 470 Ma (highest frequency) and ca. 460 Ma.

It should also be emphasized that the Zemplinic crystalline basement consists of gneisses, amphibolites, orthogneisses, and migmatites in which mineral associations indicate P–T conditions of upper amphibolite facies. Its protolith, which has been reconstructed based on the chemical composition of all rock types (major and trace elements including REE), corresponds to shales and graywackes with associated basic volcanics of tholeiitic magmatic trend and their volcaniclastic sediments (Vozárová 1991). The presence of kyanite relics in Grt–Bt gneisses indicates pressures about 1000 MPa at temperatures about 750 °C during the climax of regional metamorphism. The decompression stage was associated with the partial anatexis and migmatitization of the whole complex (Vozárová 1991; Faryad 1995; Faryad & Vozárová 1997). It may be deduced that Middle/Late Ordovician magma was mainly generated by partial melting of the Ediacaran igneous rocks. Since only very scarce evidence of the Silurian and Devonian detrital zircon ages has been recognised, a passive drifting with the Galatian ribbon microcontinent is assumed (according to Stampfli et al. 2011, 2013). The following thermal relaxation of the Zemplinic basement is connected with Devonian/Tournaisian collision events. The Zemplinic basement demonstrates low igneous activity, which is indicated by several granitoid pebbles within the Pennsylvanian–Permian basin fill (Együd 1982; Grecula & Együd 1982; Vozárová & Vozár 1988; Vozárová 1991; Faryad 1995), as well as by solitary Tournaisian/Visean detrital zircon grain (Vozárová et al. 2019a). The Carboniferous reheating is indicated by the monazite ages from paragneisses (338±22 Ma, Finger & Faryad 1999), as well as of the K/Ar ages from amphibolites (338±13 and 313±13 Ma, Faryad & Balogh 2002).

As mentioned previously, there are different views on the relationship of the Zemplinic crystalline basement. The main arguments for its belonging to the Western Carpathian orogenic system are: (i) the similarity of the protolith and the degree of metamorphism with the crystalline complexes of the Central Western Carpathians; (ii) continental sedimentary conditions for the Pennsylvanian–Permian envelope; (iii) quartzose sandstones and fine-graded oligomictic conglomerates in the basal Lower Triassic, and carbonate platform development in the Middle Triassic, consistent with the Mesozoic envelope of the crystalline complexes in the entire Central Western Carpathians (Andrusov 1968; Fusán et al. 1971; Maheľ 1986; Vozárová & Vozár 1988; Vozárová 1991; Faryad 1995; Faryad & Balogh 2002; Vozár et al. 2010). The Zemplinic connection toward the Mecsek zone of the Tisia Terrane (Tisza Unit) was suggested by Grecula & Együd (1977) and Plašienka et al. (1997, 2018). It should be noted here that the crystalline rock complexes of the Mecsek show noticeable differences compared to the Zemplinic basement, such as the presence of marbles, eclogites, and calc silicate rocks (e.g., Szederkenyi 1997, 2001; Tóth 2014 and references therein). We correlated the composition of amphibolites from Mecsek (Tóth 2014) with the BB-1 borehole amphibolites data given in this article. In general, the two groups of amphibolites do not show any clear correlation. While the chemical composition of the Mecsek amphibolites indicates an almost exclusively within-plate environment of alkaline basalts, the Zemplinic amphibolites, in addition to the OIB alkaline basalts, also show an affinity to IAT or BAAB basalts (Suppl. Fig. S1). However, the correlation is affected by the error resulting from the differences in the analytical methods used.

It must also be stated that the lithofacies of "Jakabhegy Sandstone" in the Lower Triassic, as well as the Late Triassic "Gresten facies" (Császár 1997; Haas 2001), which are typical for the Triassic development in Mecsek, are absent in the Zemplinic Unit. All these data undoubtedly indicate Zemplinic Unit affiliation with the Western Carpathian orogenic system. The question is whether Zemplinicum is a continuation of the Central Western Carpathian basements, as assumed by the above-cited authors or the Inner Western Carpathians. When taking into consideration the detrital zircon U–Pb ages that were acquired from the Meliaticum–Bôrka Nappe, as well as from the Turnaicum, Southern Gemericum, and Zemplinic units of the Pennsylvanian–Permian sedimentary sequences, these rocks are believed to have most likely been derived from the same source area (Vozárová et al. 2019a, b). Data are consistent with their derivation from the eastern peri-Gondwanan domain, with the source area of the Cadomian arc and basement rocks within the Saharan Metacraton. This would mean that the Zemplinic Unit probably belongs to the southernmost fragments of the IWC, which was displaced around the former Meliata Suture (Vozárová et al. 2019b and references therein). This interpretation is partly consistent with the suggestion of Schmid et al. (2008).

The age of regional metamorphism of the Zemplinic crystalline basement remains an unresolved question. Only a small number of identified Variscan ages indicate the rather older, pre-Variscan tectono-metamorphic events, which were

perhaps equivalent to subduction-accretion "Cenerian orogeny" according to Zurbriggen (2015, 2017). In this case, the Variscan orogeny can be interpreted mainly as overheating and rejuvenation in the extension regime, with only smaller intrusions of igneous bodies and later associated with the creation of post-tectonic Pennsylvanian–Permian sedimentary basins.

Conclusions

The conclusions may be summarised as follows:

- The Zemplinic metabasic rocks have the geochemical characteristics of both E-MORB and OIB, and were likely resulted from a depleted mantle source affected by fluid-related subduction metasomatism and crustal recycling. The geochemical parameters indicate a protolith corresponding to the extensional supra-subduction regime of the back-arc basin.
- Variable enrichment of Th, which is found only in the samples of the ***Grp-I*** amphibolites, means that the metasomatic enrichment was induced by fluid-related subduction metasomatism rather than crustal contamination.
- According to the mineral geothermobarometry and constructed phase diagrams, a substantial part of the studied amphibolites indicates P–T conditions of the upper amphibolite facies. The highest temperatures (660–725 °C) and pressures (0.78–0.88 GPa) with the association Hbl+Pl+Cpx correspond to the climax of the orogenic metamorphism of the Zemplinic crystalline basement. The exception is the two samples from the upper parts of the BB-1 borehole, with the temperatures corresponding to the lower/middle-grade amphibolite facies. They could be connected with a retrograde branch of regional metamorphism, however, tectonic contact along a ductile shear zone is not excluded.
- From the point of view of tectonic position, we consider the Zemplinic Unit to be a continuation of the Inner Western Carpathians.

Acknowledgment: The financial support of the Slovak Research and Development Agency (project ID: APVV-19-0065) and of the Scientific Grant Agency of the Ministry of Education of the Slovak Republic and the Slovak Academy of Sciences (project VEGA 2/0006/19) is gratefully appreciated. The authors would like to thank S.W. Faryad, R.M. Palin and T.M. Toth for constructive reviews and for their helpful and critical comments, which led to significant improvement of an earlier version of the manuscript.

References

Altherr R., Hepp S., Klein H. & Hanel M. 2021: Metabasic rocks from the Variscan Schwarzwald (SW Germany): metamorphic evolution and igneous protoliths. *International Journal* of *Earth Sciences (Geol. Rundschau)* 110, 1293–1319. https://doi.org/10.1007/s00531-021-02016-w

Andrusov D. 1968: Grundriss der Tektonik der Nördlichen Karpaten. *Slovak Academy Sciences*, Bratislava, pp 188.

Antić M., Peytcheva I., von Quadt A., Kounov A., Trivić B., Serafimovski T., Goran T., Gerdjikov I. & Wetzel A. 2016: Pre-Alpine evolution of segment of the North-Gondwanan margin: Geochronological and geochemical evidence from the central Serbo-Macedonian Massif. *Gondwana Research* 36, 523–544. https://doi.org/10.1016/j.gr.2015.07.020

Balintoni I., Balica C., Ducea H.N., Chen F., Hann H.P. & Şabliovschi V. 2009: Late Cambrian–Early Ordovician Gondwanan terranes in the Romanian Carpathians: A zircon U–Pb provenance study. *Gondwana Research* 16, 119–133.

Baňacký V., Vass D., Elečko M., Kaličiak M., Lexa J., Straka P., Vozár J. & Vozárová A. 1986: Geological map from the southern part of East Slovakia Lowland and Zemplín Mts., scale 1:50 000. *D. Štúr Inst. Geol.*, Bratislava.

Baňacký V., Elečko M., Kaličiak M., Straka P., Škvarka L., Šucha P., Vass D., Vozárová A. & Vozár J. 1989: Explanation to Geological map of the southern part of East Slovakia Lowland and Zemplín Mts., 1:50 000: *Dionýz Štúr Inst Geol*, Bratislava, 1–143 (in Slovak with English summary).

Bonev N., Ovtcharova-Shaltegger M., Moritz R., Marchev P. & Ulianov A. 2013: Peri-Gondwanan Ordovician crustal fragments in the high-grade basement of the Eastern Rhodope Massif, Bulgaria: evidence from U-Pb LA-ICP-MS zircon geochronology and geochemistry. *Geodinamica Acta* 23, 207–229. https://doi.org/10.1080/09853111.2013.858942

Casas J.M., Castiñeiras P., Navidad M., Liesa M. & Carreras J. 2010: New insights into the Late Ordovician magmatism in the Eastern Pyrenees: U-Pb SHRIMP zircon data from the Canigó massif. *Gondwana Research* 17, 317–324. https://doi.org/10.1016/j.gr.2009.10.006

Condie K.C. 1999: Mafic crustal xenoliths and the origin of the lower continental crust. *Lithos* 46, 95–101.

Condie K.C. 2003: Incompatible element ratios in oceanic basalts and komatiites: Tracking deep mantle sources and continental growth rates with time. *Geochemistry, Geophysics, Geosystems* 4, 1005. https://doi.org/10.1029/2002GC000333

Császár G. (Ed.) 1997: Lithostratigraphic chart of the Hungarian Stratigraphic Comission. *Hungarian Geological Inst*itute, Budapest, 1–114 (in Hungarian with English text).

Dilek Y. & Furnes H. 2011: Ophiolite genesis and global tectonics: geochemical and tectonic fingerprinting of ancient oceanic lithosphere. *Geological Society of America Bulletin* 123, 387–411. https://doi.org/10.1130/B30446.1

Dilek Y., Furnes H. & Shallo M. 2007: Supra-subduction zone ophiolite formation along the periphery of Mesozoic Gondwana. *Gondwana Research* 11, 453–475 https://doi.org/10.1016/j.gr.2007.01.005

Dostal J. & Capedri S. 1979: Rare earth elements in high-grade metamorphic rocks from the Western Alps. *Lithos* 12, 41–49.

Dörr W., Zulauf G., Gerdes A., Lahaye Y. & Kowalczyk G. 2015: A hidden Tonian basement in the eastern Mediterranean: Age constraints from U–Pb data of magmatic and detrital zircons of the External Hellenides (Crete and Peloponesus). *Precambrian Res*earch 258, 83–108. https://doi.org/10.1016/j.precamres.2014.12.015

Együd K. 1982: Sedimentology of Upper Paleozoic strata in Zemplínske vrchy Mts. *Mineralia Slovaca* 14, 385–401 (in Slovak with English summary)

Faryad S.W. 1995: Geothermometry of metamorphic rocks from the Zemplinicum. *Geologica Carpathica* 46, 113–123.

Faryad S.W. & Balogh K. 2002: Variscan pegmatite and K-Ar and Ar/Ar dating from basement rocks of the Zemplín Unit, Western Carpathians. *Acta Geologica Hungarica* 45, 193–205.

Faryad S.W. & Vozárová A. 1997: Geology and metamorphism of the Zemplinicum basement unit (Western Carpathians). In: Grecula P., Hovorka D. & Putiš M. (Eds.): Geological evolution of the Western Carpathians. *Mineralia Slovaca-Monograph*, Bratislava, 351–358.

Finger F. & Faryad S.W. 1999: A Variscan monazite age from Zemplín basement (eastern Western Carpathians). *Acta Geologica Hungarica* 42, 301–307.

Fusán O., Ibrmajer J., Plančár J. Slávik J. & Smíšek M. 1971: Geological structure of the basement of the covered part of inner West Carpathians. *Zborník Geologických Vied, rad Západné Karpaty* 15, 5–173 (in Slovak).

Fülöp I. 1994: Geology of Hungary. Paleozoic I. *Akademia Kiadó*, Budapest, 1–447 (in Hungarian).

Gärtner A., Villeneuve M., Linnemann U., El Archi A. & Bellon H. 2013: An exotic terrane of Laurussian affinity in the Mauretanides and Souttoufides (Moroccan Sahara). *Gondwana Research* 24, 687–699.

Gelinas L., Mellinger M. & Trudel P. 1982: Archaean mafic metavolcanics from the Rouyn-Noranda district, Abitibi greenstone belt, Quebec. 1. Mobility of the major elements. *Canadian Journal of Earth Sciences* 19, 2258–2275.

Grauch R.I. 1989: Rare earth elements in metamorphic rocks. In: Lipin B.R. & McKay G.A. (Eds.): Geochemistry and mineralogy of rare earth elements 21. *Mineralogical Society of America, Washington D.C.,* 147–167.

Grecula P. & Együd K. 1977: Position of the Zemplín Inselberg in the tectonic frame of Carpathians. *Mineralia Slovaca* 9, 449–462 (in Slovak with English summary).

Grecula P. & Együd K. 1982: Lithostratigraphy of Upper Paleozoic and Lower Triassic strata of the Zemplínske vrchy Mts. (SE Slovakia). *Mineralia Slovaca* 14, 221–239 (in Slovak with English summary).

Grecula P., Kaličiak M., Tözsér J. & Varga I. 1981a: Geology of the borderland between the West and East Carpathians in the work of Jan Slávik. In: Grecula P (Ed.): New data, correlations and problems. Seminary Geological days of Jan Slávik. *Spec. Issue of Slovak Geological Survey*, 17–32 (in Slovak).

Grecula P., Együd, K., Kobulský J., Fabian M. & Hodermarský J. 1981b: Zemplín Island: Polymetallic Ores and Coals. *Internal report of Slovak Geol. Survey*, 1–309 (in Slovak).

Green E., White R., Diener J., Powell R., Holland T. & Palin R. 2016: Activity composition relations for the calculation of partial melting equilibria in metabasic rocks. *Journal of Metamorphic Geology* 34, 845–869.

Haas J. 2001: Tisza Mega-Unit – Alpine evolution. In: Haas J. (Ed.): Geology of Hungary. *Eötvös University Press*, Budapest, 168–175.

Harlov D., Tropper P., Seifert W., Nijland T. & Förster H.-J. 2006: Formation of Al-rich titanite ($CaTiSiO_4O$ – $CaAlSiO_4OH$) reaction rims on ilmenite in metamorphic rocks as function of fH_2O and fO_2. *Lithos* 88, 72–84. https://doi.org/10.1016/j.lithos.2005.08.005

Hawthorne F.C., Oberti R., Harlow G.E., Maresch W.V., Martin R.F., Schumacher J.C. & Welch M.D. 2012: Nomenclature of the amphibole supergroup. *American Mineralogist* 97, 2031–2048.

Henderson B.J., Collins W.J., Murphy J.B., Gutiérrez-Alonso G. & Hand M. 2016: Gondwanan basement terranes of the Variscan Appalachian orogen: Baltican, Saharan and West African hafnium isotopic fingerprints in Avalonia, Iberia and the Armorican Terranes. In: Murphy J.B., Nance R.D. & Johnson S.T. (Eds.): Tectonic evolution of the Iberian margin of Gondwana and of correlative region. A celebration of the career of Cecilio Quesada. *Tectonophysics* 681, 278–304.

Hofmann A.W. 1997: Mantle geochemistry: the message from oceanic volcanism. *Nature* 385, 219–229.

Holland T. & Blundy J. 1994: Non-ideal interactions in calcic amphiboles and their bearing on amphibole-plagioclase thermometry. *Contributions to Mineralogy and Petrology*. 116, 433–447. https://doi.org/10.1007/BF00310910

Holland T.J.B. & Powell R. 2011: An improved and extended internally consistent thermodynamic dataset for phases of petrological interest, involving a new equation of state for solids. *Journal of Metamorphic Geology* 29, 333–383.

Hollocher K., Robinson P., Walch E. & Roberts D. 2012: Geochemistry of amphibolite-facies of volcanics and gabbros of the Stóren Nappe in extensions west and southwest of Trondheim, Western Gneiss Region, Norway: A key to correlations and palaeotectonic settings. *American Journal of Science* 312, 357–416. https://doi.org/10.2475/04.2012.01

Humphris S.E. 1984: The mobility of the rare earth elements in the crust. In: Henderson P. (Ed.): Developments in Geochemistry 2 – Rare Earth Element Geochemistry. *Elsevier*, Amsterdam, 317–342.

Kröner A. & Stern R.J. 2004: Pan-African Orogeny. Encyclopaedia of Geology, Vol 1. *Elsevier*, Amsterdam, 1–12.

Ilnicki S., Szcepański J. & Pin Ch. 2020: Tholeiitic- and boninite – series metabazites of the Nové Město Unit and northern part of the Zábřeh Unit (Orlica-Śnieźnik Dome, Bohemian Massif): petrogenesis and tectonic significance. *International Journal of Earth Sciences (Geol. Rundsch.)* 109, 1247–1271. https://doi.org/10.1007/s00531-020-01845-5

John T., Scherer E.E., Haase K. & Schenk V. 2004: Trace element fractionation during fluid-induced eclogitization in a subducting slab: trace element and Lu-Hf-Sm-Nd isotope systematics: *Earth and Planetary Science Letters* 227, 441–456. https://doi.org/10.1016/j.epsl.2004.09.009

Kisházi P. & Ivancsics J. 1988: Contribution to the petrology of crystalline schists in the Zemplín structure. *Bulletin of Hungarian Geological Soc*iety 2, 109–124 (in Hungarian).

Lelkes-Felvári Gy., Árkai P. & Sassi F.P. 1996: Main features of the regional metamorphic events in Hungary: A review. *Geologica Carpathica* 47, 257–270.

Liao Y., Wei Ch. & Rehman H.U. 2021: Titanium in calcium amphibole: Behaviour and thermometry. *American Mineralogist* 106, 180–191. https://doi.org/10.2138/am-2020-7409

Linnemann U., Pereira F., Jeffries T.E., Drost K. & Gerdes A. 2008: The Cadomian orogeny and the opening of the Rheic Ocean: the diachrony of geotectonic processes constrained by LA-ICP-MS U–Pb zircon dating (Ossa-Morena and Saxo-Thuringian zones, Iberian and Bohemian massifs). *Tectonophysics* 461, 21–43.

Maheľ M. 1986: Geological structure of the Czechoslovak Carpathians, Part 1: Paleoalpine units. Monograph, *Veda Publishing House*, Bratislava, 1–503 (in Slovak).

MacGeehan P.J. & MacLean W.H. 1980: An Archaean sub-seafloor geothermal system, 'calc-alkali' trends, and massive sulphide genesis. *Nature* 286, 767–771.

Magyar J. 1969: Geology and petrography of the crystalline window of the Zemplinicum and the surrounding formations. *Manuscript, Comenius University*, Bratislava, 1–78 (in Slovak).

Martinez F., Okino K., Ohara Y., Reysenbach A.-L. & Goffredi S.K. 2007: Back-arc basins. *Oceanography* 20, 116–127. https://doi.org/10.5670/oceanog.2007.85

McDonough W.F. & Sun S-S. 1995: The composition of the Earth. *Chemical Geology* 120, 223–253.

Molina J.F., Moreno J.A., Castro A., Rodríguez C. & Fershtater G.B. 2015: Calcic amphibole thermobarometry in metamorphic and igneous rocks: New calibrations based on plagioclase/amphibole Al-Si partitioning and amphibole/liquid Mg partitioning. *Lithos* 232, 286–305. https://doi.org/10.1016/j.lithos.2015.06.027

Montanini A., Tribuzio R. & Vernia L. 2008: Petrogenesis of basalts and gabbros from an ancient continent-ocean transition (External Liguride ophiolites, Northern Italy). *Lithos* 101, 453–479. https://doi.org/10.1016/j.lithos.2007.09.007

Morimoto N., Fabries J., Ferguson A.K., Ginzburg I.V., Ross M., Seifert F.A., Zussman J., Aoki K. & Gottardi G. 1988: Nomenclature of pyroxenes. *American Mineralogist* 73, 1123–1133.

Murphy J.B. & Nance R.D. 1989: Model for evolution of the Avalonian–Cadomian belt. *Geology* 17, 735–738.

Nance R.D., Murphy J.B. & Keppie J.D. 2002: A Cordilleran model for the evolution of Avalonia. *Tectonophysics* 352, 11–31.

Neubauer F. 2002: Evolution of late Neoproterozoic to early Palaeozoic tectonic elements in central and southeast European alpine mountain belts: review and synthesis. *Tectonophysics* 352, 87–103.

Palin R.M., Weller O.M., Waters D.J. & Dyck B. 2016: Quantifying geological uncertainty in metamorphic phase equilibria modelling; a Monte Carlo assessment and implications for tectonic interpretations. *Geoscience Frontiers* 7, 591–607. https://doi.org/10.1016/j.gsf.2015.08.005

Pantó G. 1965: Pre-Tertiary formation of the Tokaj Mts. *Annual Report Hungarian Geological Institute* 1963, 277–241 (in Hungarian with English summary)

Pantó G., Kovách Á., Balogh K. & Sámsoni Z. 1967: Rb–Sr check of Assyntian and Caledonian metamorphism and igneous activity in NE Hungary. *Acta Geologica Hungarica* 11, 279–282.

Pearce J.A. 1976: Statistical analysis of major element patterns in basalts. *Journal of Petrology* 17, 15–43.

Pearce J.A. 1996: A User's Guide to basalt Discrimination Diagrams. In: Wymann D.A. (Ed.): Trace Element geochemistry of volcanic rocks: Applications for Massive Sulphide Exploration. *Geological Association of Canada. Short Course Note* 12, 79–113.

Pearce J.A. 2008: Geochemical fingerprinting of oceanic basalts with applications to ophiolite classification and to search for Archean oceanic crust. *Lithos* 100, 14–43.

Pearce J.A. 2014: Immobile element fingerprinting of ophiolites. *Elements* 10, 101–108.

Pearce J.A. & Peate D.W. 1995: Tectonic implications for the composition of volcanic arc magmas. *Annual Review of Earth and Planetary Sciences* 23, 251–285.

Pearce J.A. & Stern R.J. 2006: Origin of back-arc basin magmas: trace element and isotope perspectives. *AGU Geophys. Monogr. Ser.* 166, 63–86.

Plašienka D. 2018: Continuity and episodicity in the early Alpine tectonic evolution of the Western Carpathians: How large-scale processes are expressed by the orogenic architecture and rock record data. *Tectonics* 37, 2029–2079.

Plašienka D., Grecula P., Putiš M., Kováč M. & Hovorka D. 1997: Evolution and structure of the Western Carpathians: an overview: In: Grecula P., Hovorka D. & Putiš M. (Eds.): Geological Evolution of the Western Carpathians. *Mineralia Slovaca–Monograph*, Bratislava, 1–24.

Powell R. & Holland T.J.B. 2008: On thermobarometry. *Journal of Metamorphic Geology* 26, 155–179.

Putiš M., Sergeev S., Ondrejka M., Larionov A., Siman P., Spišiak J., Uher P. & Paderin I. 2008: Cambrian-Ordovician metaigneous rocks associated with Cadomian fragments in the West-Carpathian basement dated by SHRIMP on zircons: a record from the Gondwana active margin setting. *Geologica Carpathica* 59, 3–18.

Rampone E., Romairone A., Abouchami W., Piccardo G.B. & Hofmann A.W. 2005: Chronology, petrology, and isotope geochemistry of the Erro-Tobbio peridotites (Ligurian Alps, Italy): records of late Palaeozoic lithospheric extension. *Journal of Petrology* 46, 799–827. https://doi.org/10.1093/petrology/egi001

René M. 2008: Titanite-ilmenite-magnetite phase relations in amphibolites of the Chýnov area (Bohemian Massif, Czec Republic). *Acta Geodynamica et Geomaterialia* 5, 239–246.

Ridolfi F., Renzulli A. & Pueriny M. 2010: Stability and chemical equilibrium of amphibole in calc-alkali magma: an overview, new thermobarometric formulations and application to subduction-related volcanoes. *Contribution to Mineralogy and Petrology* 160, 45–66. https://doi.org/10.1007/s00410-009-0465-7

Roger E., Respaut J.P., Brunel M., Matte Ph. & Paquette J.L. 2004: Premiere datation U–Pb des orthogneiss oeilles de la zone axiale de la Montgane Noire (Sud du Massif central): nouveaux temains du magmatisme ordovicien dans la chalne varisque. *Comptes Rendus Geoscience* 336, 19–28.

Rollinson H.R. 1993: Using geochemical data: evaluation, presentation, interpretation. *Longman*, Singapore, 1–352.

Rudinec R. & Slávik J. 1970: Geological structure of the basement of Neogene of East Slovakia. *Geologické Práce Správy* 53, 145–157 (in Slovak with English summary).

Rudnick R. L. 1995: Making continental crust. *Nature* 378, 571–578.

Saccani E. 2015: A new method of discriminating different of post-Archean ophiolitic basalts and their tectonic significance using Th–Nb and Ce–Dy–Yb systematics. *Geoscience Frontiers* 6, 481–501.

Saccani E., Bortolotti V., Marroni M., Pandolfi L., Photiades A. & Principi G. 2008: The Jurassic association of back-arc basin ophiolites and calc-alkaline volcanics in the Guevgueli Complex (northern Greece): implication for the evolution of the Vardar Zone. *Ofioliti* 33, 209–227.

Saunders A.D., Norry M.J. & Tarney J. 1988: Origin of MORB and chemically depleted mantle reservoirs: trace element constraints. *Journal of Petrology, Special Volume* 1, 415–445. https://doi.org/10.1093/petrology/Special_Volume.1.415

Shervais J.W. 1982: Ti–V plots and the petrogenesis of modern and ophiolitic lavas. *Earth and Planetary Science Letters* 59, 101–118.

Schmid S.M., Bernoulli D., Fügenschuh B., Matenco L., Schefer S., Schuster R., Tischler M. & Ustaszewski K. 2008: The Alpine-Carpathian-Dinaridic orogenic system: correlation and evolution of tectonic units. *Swiss Journal of Geoscience* 100, 139–183. https://doi.org/10.1007/s00015-008-1247-3

Sirevaag H., Jacobs J., Ksienzyk A.K., Rocchi S., Paoli G., Jørgensen H. & Košler J. 2016: From Gondwana to Europe: The journey of Elba Island (Italy) as recorded by U–Pb detrital zircon ages of Paleozoic metasedimentary rocks. *Gondwana Research* 38, 273–288. https://doi.org/10.1016/j.gr.2015.12.006

Slávik J. 1976: Zemplinicum – a possible new tectonic unit of the Central West Carpathians. *Geologické Práce Správy* 65, 7–19 (in Slovak with English summary).

Stampfli G.M., von Raumer J. & Wilhem C. 2011: The distribution of Gondwana-derived terranes in the Early Palaeozoic. In: Gutiérrez-Marco J.C., Rábano I. & García-Bellido D. (Eds.): Ordovician of the World. *Cuadernos del Museo Geominero* 14, 567–574.

Stampfli G.M., Hochard C., Vérard C., Wilhem C. & von Raumer J. 2013: The formation of Pangea. *Tectonophysics* 593, 1–19.

Stephan T., Kroner U., Romer R.L. & Rösel D. 2019: From a bipartite Gondwanan shelf to an arcuate Variscan belt: The early Paleozoic evolution of northern Peri-Gondwana. *Earth-Science Reviews* 192, 491–512.

Sun S-S. & McDonough W.F. 1989: Chemical and isotope systematic of oceanic basalts implications for mantle composition and processes. In: Sounders A.D. & Norry M.J. (Eds.): Magmatism in ocean basins. *Geological Society London, Special Publication* 42, 313–345.

Szederkenyi T. 1997: Metamorphic formations of the Hungarian part of the Tisza Unit (Tisia Composite Terrane) and their correlation. In: Haas J. (Ed.): Fülöp József emlékkönyv. *Akad. Kiadó*, Budapest, 133–147 (in Hungarian).

Szederkenyi T. 2001: Tisza Mega-unit. Pre-Alpine evolution. In: Haas J. (Ed.): Geology of Hungary. *Eötvös University Press*, Budapest, 148–168.

Tischendorf G., Förster H.-J., Gottesmann B. & Rieder M. 2007: True and brittle micas: composition and solid-solution series. *Mineralogical Magazine* 71, 285–320.

Tóth M.T. 2014: Geochemistry of the Görcsöny Ridge amphibolites (Tisza Unit, SW Hungary) and its geodynamic consequences. *Geologica Croatica* 67, 17–32. https://doi.org/10.4154/gc.2014.02

Turner S., Rushmer T., Reagan M. & Moyen J.-F. 2014: Heading down early on? Start of subduction on Earth. *Geology* 42, 139–142. https://doi.org/10.1130/G34886.1

von Raumer J.F., Bussy F., Schaltegger U., Schulz B. & Stampfli G.M. 2013: Pre-Mesozoic alpine basements-their place in the European Palaeozoic framework. *Geological Society of America Bulletin* 125, 89–108. https://doi.org/10.1130/B30654.1

Vozár J., Hanzel V., Vozárová A. & Zlínska A. 1986: Data processing from the borehole BB-1 (650 m). *Manuscript*, *Archives of the State Dionýz Štúr Geological Institute*, Bratislava (in Slovak).

Vozár J., Ebner F., Vozárová A., Haas J., Kovács S., Sudar M., Bielik M. & Péró Cs. (Eds.) 2010: Variscan an Alpine terranes of the Circum-Pannonian Region. *Monograph Geological Institute of Slovak Academy of Sciences*, Bratislava, 7–233

Vozárová A. 1989: Petrology of crystalline rocks of Zemplinicum (West Carpathians). In: Papanikolaou D. & Sassi F.P. (Eds.): IGCP No. 276, Newsletter No. 1, *Geological Society of Greece, Special Publication* 1, 97–104.

Vozárová A. 1991: Petrology of crystalline rocks of Zemplinicum (West Carpathians). *Západné Karpaty, Séria Mineralogy, Petrography, Geochemistry, Metalogeny* 14, 7–59 (in Slovak with English summary).

Vozárová A. & Vozár J. 1988: Late Paleozoic in West Carpathians. *Monograph*, *Dionýz Štúr Geological Institute*, Bratislava, 1–314.

Vozárová A., Šarinová K., Larionov A., Presnyakov S. & Sergeev S. 2010: Late Cambrian /Ordovician magmatic arc type volcanism in the Southern Gemericum basement, Western Carpathians, Slovakia: U–Pb (SHRIMP) data from zircons. *International Journal of Earth Sciences (Geol. Rundsch.)* 99 (Suppl 1), 17–37. https://doi.org/10.1007/s00531-009-0454-0

Vozárová A., Rodionov N., Šarinová K. & Presnyakov S. 2017: New zircon ages on the Cambrian–Ordovician volcanism of the Southern Gemericum basement (Western Carpathians, Slovakia): SHRIMP dating, geochemistry and provenance. *International Journal of Earth Sciences (Geol. Rundsch.)* 106, 2147–2170. https://doi.org/10.1007/s00531-016-1420-2

Vozárová A., Larionov A., Šarinová K., Rodionov N., Lepekhina E., Vozár J. & Paderin I. 2019a: Clastic wedge provenance in the Zemplinicum Carboniferous–Permian rocks using the U–Pb zircon age dating (Western Carpathians, Slovakia). *International Journal of Earth Sciences (Geol. Rundsch.)* 108, 115–135. https://doi.org/10.1007/s00531-018-1654-3

Vozárová A., Rodionov N., Šarinová K., Lepekhina E., Vozár J., Paderin I. 2019b: Detrital zircon U–Pb geochronology of Pennsylvanian–Permian sandstones from the Turnaicum and Meliaticum (Western Carpathians, Slovakia): provenance and tectonic implication. *International Journal of Earth Sciences (Geol. Rundsch.)* 108, 1793–1715. https://doi.org/10.1007/s00531-019-01733-7

Warr L.N. 2021: IMA-CNMNC approved mineral symbols. *Mineralogical Magazine* 85, 291–320. https://doi.org/10.1180/mgm.2021.43

White R.W., Powell R. & Holland T.J.B. 2001: Calculation of partial melting equilibria in the system Na_2O–CaO–K_2O–FeO–MgO–Al_2O_3–SiO_2–H_2O (NCKFMASH). *Journal of Metamorphic Geology* 19, 139–153.

White R.W., Powell R. & Holland T.J.B. 2007: Progress relating to calculation of partial melting equilibria for metapelites. *Journal of Metamorphic Geology* 25, 511–527. https://doi.org/10.1111/j.1525-1314.2007.00711.x

White R.W., Powell R., Holland T., Johnson T. & Green E. 2014: New mineral activity composition relations for thermodynamic calculations in metapelitic systems. *Journal of Metamorphic Geology* 32, 261–286.

Winchester J.A. & Floyd P.A. 1977: Geochemical discrimination of different magma series and their differentiation products using immobile elements. *Chemical Geology* 20, 325–343.

Woelki D., Regelous M., Haase K.H., Romer H.W. & Beier Ch. 2018: Petrogenesis of boninitic lavas from Troodos Ophiolite and comparison with Izu-Bonin-Mariana fore-arc crust. *Earth and Planetary Science Letters* 498, 203–214. https://doi.org/10.1016/j.epsl.2018.06.041

Wood D.A. 1980: The application of a Th-Hf-Ta diagram to problems of tectonomagmatic classification and to establishing the nature of crustal contamination of basaltic lavas of the British Tertiary Volcanic Province. *Earth and Planetary Science Letters* 50, 11–30.

Xiang H. & Connolly J.A.D. 2022: GeoPS: An interactive visual computing tool for thermodynamic modelling of phase equilibria. *Journal of Metamorphic Geology* 40, 243–255. https://doi.org/10.1111/jmg.12626

Xirouchakis D. & Lindsley D. H. 1998: Equilibria among titanite, hedenbergite, fayalite, quartz, ilmenite, and magnetite: Experiments and internally consistent thermodynamic data for titanite. *American Mineralogist* 83, 712–725.

Zurbriggen R. 2015: Ordovician orogeny in the Alps: a reappraisal. *International Journal of Earth Sciences (Geol. Rundsch.)* 104, 335–350. https://doi.org/10.1007/s00531-014-1090-x

Zurbriggen R. 2017: The Cenerian orogeny (Early Paleozoic) from the perspective of the Alpine region. *International Journal of Earth Sciences (Geol. Rundsch.)* 106, 517–529. https://doi.org/10.1007/s00531-016-1438-5

Electronic supplementary material is available online:
Supplementary Tables S1–S5 at http://geologicacarpathica.com/data/files/supplements/GC-73-6-Vozarova-Suppl_TablesS1-S5.xlsx
Supplementary Fig S1 at http://geologicacarpathica.com/data/files/supplements/GC-73-6-Vozarova-Suppl_Fig_S1.jpg

Supplement

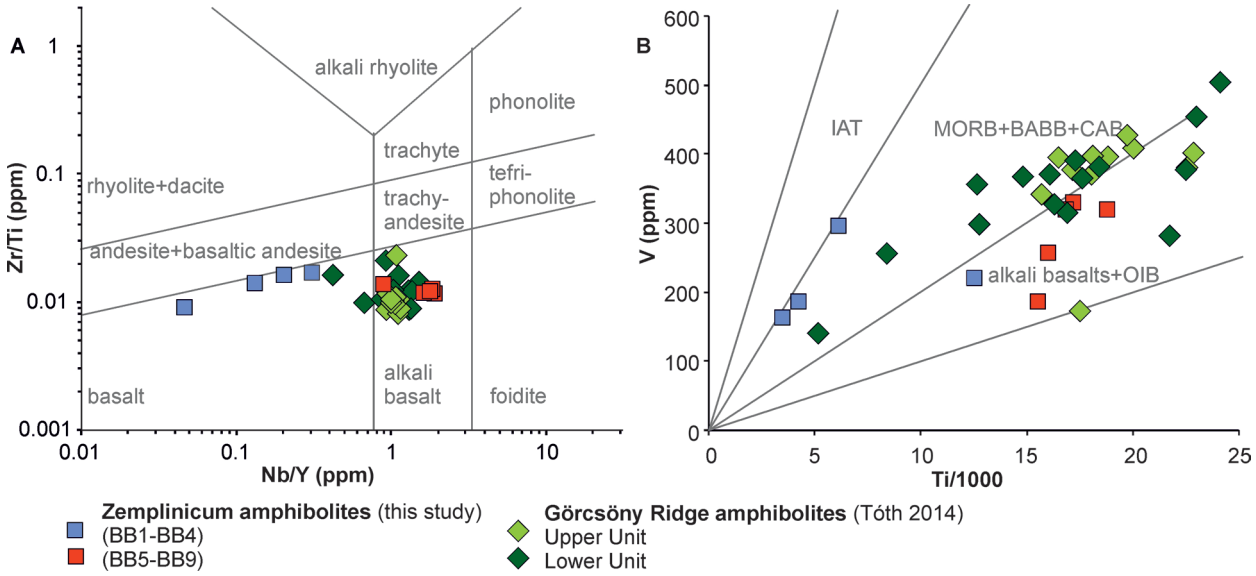

Fig S1. Correlation of the Zemplinic and Mecsek metabasic rocks: **A** — V vs. Ti/1000 metabasalt classification (from Shervais 1982); **B** — Zr/Ti versus Nb/Y from Pearce (1996) diagram, revised by Winchester & Floyd (1977).